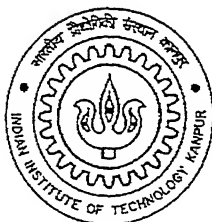


# CO-OPERATIVE DEFORMATION OF GLASS-METAL LAMINATE

*A Thesis Submitted*  
in Partial Fulfilment of the Requirements  
for the Degree of  
Master of Technology

*by*  
Anirban Guha



*to the*  
DEPARTMENT OF MATERIALS AND METALLURGICAL ENGINEERING  
INDIAN INSTITUTE OF TECHNOLOGY KANPUR

May, 1998

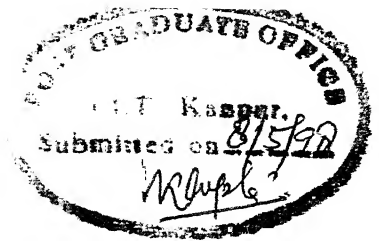
1 3 JUL 1998  
CENTRAL LIBRARY  
I. I. T. KANPUR

---

Acc. No. A 125717

MME-1998-M-GUH-CO

# CERTIFICATE



It is certified that the work contained in the thesis entitled Co-operative deformation behaviour of glass-metal laminate by Anirban Guha, has been carried out under my supervision and to the best of my knowledge this work has not been submitted elsewhere for a degree.

Dr. V. S. R. Murthy  
Associate Professor  
Department of Materials and  
Metallurgical Engg.  
Indian Institute of Technology,  
Kanpur.

May, 1998

*This thesis is dedicated to*

*MY ALL FRIENDS....*



# Acknowledgements

I am deeply ingratiated to my supervisor, Dr. V. S. R. Murthy who have provided the much needed academic guidance with the firmness of a teacher and accessibility of a friend. I thank this gentleman to have put all the needed resources at my disposal. I sincerely appreciate the pains he took to scrutinise even the minutest of details while helping me bring this work to its final shape.

I can't ignore the cooperation of all my friends who have in their varying capacities helped me in someway or the other with this thesis. I want to thank specially Mr. Satyam Suwas. I cann't forget to thank Pradyot, Sudip, Dhiman, Munshi, Koushik, Kamalesh, Brijesh, Robert, Mallikarjun, Patro, Tiwari, G. B. Babu, Santanu, Dr. Daniel, Mr. and Mrs. A. Haldar. Finally I wish to extend my gratitude to Mr. Prasad and Mr. Malvya of Ceramics lab for their support.

Anirban Guha

IIT Kanpur

May,1998

# Abstract

'Superplasticity' is a well-established phenomenon in metals and their alloys. Recently advanced materials like ceramics, intermetallics and composites are also shown to exhibit superplasticity. Further a good understanding also has been obtained on the flow behaviour of metal-metal laminates. However, there is no work has been carried out on co-operative deformation of ceramic-metal laminates. Hence, in the present investigation the flow behaviour of glass-metal laminate has been explored at elevated temperatures.

The superplasticity in Zn-Al eutectoid alloy is a well-established fact with recorded maximum elongation of 2900%. It can be processed at fairly low-temperatures. Ceramic phase is chosen to be glass because at similar temperatures where Zn-Al alloy deforms, it exhibits perfect Newtonian behaviour with strain rate sensitivity index equals to unity. To study the deformation behaviour of laminates, sodium-alumino-borosilicate glass was diffusion bonded with hypereutectoid Zn-Al alloy to form glass-metal laminates (3 layers of metal and 2 layers of glass). The interface between alloy and glass was found to be purely mechanical with an interfacial strength of 0.9MPa. The deformation behaviour of laminates was studied at four different temperatures e.g. 160°C, 180°C, 200°C and 220°C. Generally in laminates, the flow stress decreased with increasing temperature. The strain rate sensitivity values varied from  $\sim 0.2$  to  $\sim 0.55$  depending on the strain rate. The flow behaviour was dominated by Zn-Al alloy and different elongations were observed in metal layers. However, glass layer did not show any deformation at these temperatures, but underwent extreme cracking perpendicular to tensile direction. The glass within the laminate underwent devitrification and rhombohedral  $Al_2O_3$  has crystallized. This was confirmed by both DTA and X-ray diffraction studies. As a result of crystallisation, glass which was supposed to have exhibited Newtonian behaviour deforms as a brittle solid. Moreover, the thermal expansion co-efficient difference between the residual glass and crystalline phase generates microcracking in the glass. The elongation values are mainly dictated by the alloy. At 160°C an elongation of  $\sim 90\%$  was observed whereas at 220°C an elongation value of  $\sim 330\%$  was recorded. Activation energy of laminate deformation is estimated as 161KJ/mol.

To obtain further insight into the problem, the flow behaviour of individual components viz. glass and Zn-Al alloy was taken up and tests were conducted at the same test temperatures as in the case of laminates. Zn-Al alloy exhibited similar features that were observed in the laminate. The glass behaves like brittle solid in the same temperature range. But it becomes perfect Newtonian fluid at  $\sim 520^{\circ}\text{C}$ . The main limitation is that there are not many glass compositions which are stable with high glass transition temperature. Secondly, the interfacial bond strength has to be high for co-operative deformation. In the present case, the interfacial bond strength is poor. It could be improved either by pre-oxidation of metal or by using an interlayer which is compatible with glass and metal.

# Contents

Title	i
Certificate	ii
Acknowledgements	iv
Abstract	v
Contents	vii
List of Figures	x
List of Tables	xii
1 Introduction	1
1.1 References . . . . .	3
2 Literature Review	4
2.1 Introduction . . . . .	4
2.2 Laminated Composite Fabrication methods . . . . .	5
2.2.1 Bonded laminates . . . . .	5
2.2.2 Deposited Laminates . . . . .	9
2.2.3 Spray Formed Laminates . . . . .	9
2.3 Properties of laminates . . . . .	10
2.3.1 General Constitutive Equation . . . . .	10

2.3.2	Room Temperature Properties . . . . .	13
2.3.3	Thermal Expansion Co-efficient . . . . .	17
2.3.4	Fracture Toughness of laminated Ceramic composite with ductile re- inforcements . . . . .	17
2.3.5	Glass-metal bonding and their interface . . . . .	22
2.3.6	High temperature mechanical properties of laminates . . . . .	23
2.4	Characterization of laminated composites . . . . .	27
2.4.1	Testing of superplastic property . . . . .	29
2.5	Individual properties . . . . .	31
2.5.1	Superplasticity in aluminium alloys . . . . .	31
2.5.2	Zn-Al alloy system . . . . .	31
2.5.3	Deformation of glass . . . . .	34
2.6	Scope of this work . . . . .	34
2.7	References . . . . .	36
<b>3</b>	<b>Experimental Details</b> . . . . .	<b>40</b>
3.1	Selection of materials . . . . .	40
3.2	Preparation of metal strips . . . . .	40
3.3	Preparation of glass powder . . . . .	41
3.4	Preparation of laminates . . . . .	42
3.5	Characterization of laminates . . . . .	42
3.5.1	Differential Thermal Analysis . . . . .	42
3.5.2	X-ray Diffraction . . . . .	42
3.5.3	Microstructural study . . . . .	43
3.5.4	High temperature testing . . . . .	44
3.6	Reference . . . . .	44
<b>4</b>	<b>Results and discussion</b> . . . . .	<b>45</b>
4.1	Introduction . . . . .	45
4.2	Characterisation of laminate . . . . .	46

4.2.1	Interface of laminate . . . . .	46
4.2.2	Flow behaviour of laminate . . . . .	48
4.3	Characterisation of glass . . . . .	52
4.3.1	DTA and X-ray diffraction . . . . .	53
4.3.2	Flow behaviour of glass . . . . .	56
4.4	Characterisation of Zn-Al alloy . . . . .	57
4.4.1	Microstructural Study . . . . .	57
4.4.2	Flow behaviour of Zn-Al alloy . . . . .	57
4.5	References . . . . .	63
5	Summary . . . . .	64
6	Suggestion for future work . . . . .	65

# List of Figures

2.1	Deformation response of laminates during press bonding (a) strainrate-stress response; (b) isostrain behaviour; (c) isostress behaviour . . . . .	8
2.2	Lamina principal axis . . . . .	11
2.3	Bending geometry in the x-z plane (a) initial cross section; (b) deformed cross section . . . . .	12
2.4	Experimental tensile elongation to fracture $e_f$ of thick layer laminated UHCS/Brass composites containing 50vol% of each component compared with prediction based on rule-of-mixtures . . . . .	14
2.5	Schematic diagram of (a) uniform and (b) nonuniform laminates loaded in transverse bending . . . . .	15
2.6	Schematic diagram illustrating the range of stress-strain characteristics exhibited by ceramic matrix composites . . . . .	18
2.7	Load-deflection curves measured for flexure strength of laminates with different thicknesses of nickel layers and comparison with that of monolithic alumina . . . . .	19
2.8	Schematic depiction of the stress field at an interfacial crack. The value of $\varphi$ can vary from $0^\circ$ (pure modelI, crack opening) to $90^\circ$ (pure modelII, shearing) . . . . .	20
2.9	Geometry of crack deflection at an interface . . . . .	21
2.10	Schematic representations are shown in above figure of: (a) isotrain testing orientation of the laminated composites, (b) mechanical analogy of the deformation of a two-component composite; in the isostrain orientation the analogy consists of two dashpots arranged in parallel and subjected to a stress $\sigma$ , (c) the predicted strain rate-stress behaviour of each of the two components as well as the overall behaviour of the laminated composite. As may be seen, the behaviour of the stronger of the two components. . . . .	26
2.11	Schematic illustration of the two different procedures used to logarithmically plot the mechanical data of superplastic materials : stress vs. strain rate(left) and strain rate vs. stress(right) . . . . .	29
2.12	Schematic phase diagram of Zn-Al system. . . . .	31

2.13	Elongation to failure(upper) and flow stress(lower) vs. initial strain rate for Zn-22%Al having a grain size of $2.5\mu\text{m}$ tested in the temperature range from $150^{\circ}\text{C}$ to $230^{\circ}\text{C}$ . . . . .	32
2.14	Linear variation of stress with strain rate in Zn-22Al eutectoid. . . . .	33
2.15	Lines from the deformation maps of some (a) non-metals and (b) metals for a deformation rate of $10^{-7}/\text{sec}$ . . . . .	35
2.16	Variation with temperature of the viscosity of some commercial glasses . . . .	35
3.1	Plan and elevation of the tensile sample : (a) metallic; (b) glass-metal laminate. .	41
3.2	Interfacial bond strength measurement of Na-alumino-borosilicate glass-Zn-Al alloy laminate. . . . .	43
4.1	Micrographs of laminate showing different layers of components and their interface. . . . .	47
4.2	True stress-true strain rate plot for laminate at $160^{\circ}\text{C}$ , $180^{\circ}\text{C}$ , $200^{\circ}\text{C}$ and $220^{\circ}\text{C}$	49
4.3	m - log $\dot{\epsilon}$ plot for laminate at $160^{\circ}\text{C}$ , $180^{\circ}\text{C}$ , $200^{\circ}\text{C}$ and $220^{\circ}\text{C}$ . . . . .	50
4.4	Comparison of % elongation values of laminate. . . . .	51
4.5	Gradual failure of metal layers in laminate. . . . .	51
4.6	DTA result of (a) original glass powder, and glass heat-treated for 1 hour at (b) $280^{\circ}\text{C}$ , (c) $550^{\circ}\text{C}$ and (d) $1000^{\circ}\text{C}$ . . . . .	54
4.7	X-ray diffraction plots of the glass powder : (a) tested in compression, (b) heat-treated at $280^{\circ}\text{C}$ , (c) heat-treated at $550^{\circ}\text{C}$ and (d) heat-treated at $1000^{\circ}\text{C}$ , (e) taken from laminate. . . . .	55
4.8	True stress-true strain rate plot for Sodium alumino-borosilicate glass at $520^{\circ}\text{C}$ and $530^{\circ}\text{C}$ . . . . .	56
4.9	m - log $\dot{\epsilon}$ plot for Sodium alumino-borosilicate glass at $520^{\circ}\text{C}$ and $530^{\circ}\text{C}$ . . .	57
4.10	Microstructure of Zn-Al alloy (a) recrystallised; (b) rolling plane; (c) & (d) other two transverse plane. . . . .	58
4.11	Continued..Microstructure of Zn-Al alloy (a) recrystallised; (b) rolling plane; (c) & (d) other two transverse plane. . . . .	59
4.12	True stress-true strain rate plot for Zn-Al at $160^{\circ}\text{C}$ , $180^{\circ}\text{C}$ , $200^{\circ}\text{C}$ and $220^{\circ}\text{C}$	60
4.13	m - log $\dot{\epsilon}$ plot for Zn-Al at $160^{\circ}\text{C}$ , $180^{\circ}\text{C}$ , $200^{\circ}\text{C}$ and $220^{\circ}\text{C}$ . . . . .	60
4.14	Comparison of % elongation values of alloy. . . . .	61



4.15 True stress-true strain plot for Zn-Al at 160°C with cross-head velocity 0.5mm/min,  
gauge length 3.9mm . . . . . 62

# List of Tables

2.1	Typical fracture energy and fracture toughness values for various materials[24]	18
2.2	Superplasticity in laminated composite . . . . .	27
2.3	Testing of laminate properties [41, 42, 43] . . . . .	28
2.4	Superplasticity in Al-alloys . . . . .	30
2.5	Superplasticity in Zn-22Al alloy[61] . . . . .	33
3.1	Relevant properties of glasses and alloys . . . . .	41
4.1	% elongation of laminate at various temperature and initial strain rate . . .	50

# Chapter 1

## Introduction

“Demands on materials imposed by today’s advanced technologies have become so diverse and severe that they often cannot be met by simple single-component materials acting alone. It is frequently necessary to combine several materials into a composite to which each constituent not only contributes its share, but whose combined action transcends the sum of the individual properties, and provides new performance unattainable by the constituents acting alone. Space vehicles, heat shields, rocket propellants, deep submergence vessels, buildings, vehicles for water and land transport, aircraft, pressure tanks and many others impose requirements that are best met, and in many instances met only by composite materials”. These few sentences from a basic survey on composite materials by A.G.H.Dietz[1]<sup>1</sup> explain the indispensable requirement of composite materials in engineering and scientific community and also in whole society. Among various kind of composite materials, we will restrict our discussion to only laminated composite materials.

A laminated composite consists of two or more layers or laminae of different materials completely bonded to each other so as to yield a composite material whose properties differ from and are more desirable than those of its constituents. By careful selection of these layers, laminated composite may be designed to have outstanding properties for a wide variety of special applications, which may require better mechanical properties, or corrosion resistance or enhanced thermal or electrical characteristics. The ultimate tailoring of properties can be done by using functionally gradient materials. Functionally gradient materials are used to produce components featuring engineered gradual transitions in microstructure and/or compositions. the presence of which is motivated by functional performance requirements that vary with location within the part. With functionally gradient materials, these requirements are met in a manner that optimises the overall performance of the component.

<sup>1</sup>references are given at the end of each chapter

For example, the body of a gear must be tough, whereas its surface must be hard and wear resistant[2].

Laminated composites have a long history of usefulness. Dietz[3] and Smith[4] have presented some fascinating examples of the early use of laminated composites. Laminating to improve the properties of materials or to combine several materials into one is not new, but the rapid expansion of the principle into a great variety of different applications is relatively recent and is accelerating at an increasingly rapid pace. To a large degree, therefore, it represents something new in the field of materials. When forming of laminated composite in a definite shape is considered, superplasticity gives an economically feasible solution.

Superplasticity, the ability of certain materials to undergo very large tensile strains, was first described in 1912[5]. It became the subject of intense research in the early 1960s following a review of Soviet work and the illustration of the potential commercial application of superplasticity. Though no universally accepted definition of superplasticity exists, the following version was proposed and accepted at the 1991 International Conference on Superplasticity in Advanced Materials(ICSAM-91) held in Osaka, Japan[6] :

Superplasticity is the ability of a polycrystalline materials to exhibit, in a generally isotropic manner, very high tensile elongations prior to failure.

Unlike conventional materials, superplastic materials are extremely resistant to neck formation when deformed in tension. This behaviour is derived from the high strain rate sensitivity of flow stress. In the area of superplastic laminates, studies have been carried out mainly in ultrahigh carbon(UHC) steel-based laminates. In fact, several UHC steel laminates consisting of superplastic and non-superplastic components have been found to be superplastic[7].

In this study, glass which is visco-elastic in the vicinity of its softening point is used along with superplastic Al-alloys. Glass behaves like ideal Newtonian fluid having strain rate sensitivity index( $m = 1$ ) while superplastic Al-alloys(eutectoid  $Zn - 22\%Al$ ) have high strain rate sensitivity of flow stress. Diffusion bonded glass-metal laminate is tested in tensile mode and the combined deformation behaviour of a laminated system is examined in this study.

This study may find some applications in the places where forming of a glass-metal composite part is indispensable option. Bonded glass-metal components are already in use in the field of lamp manufacturing, porcelain enamelling and ceramic-ware glazing and also in microelectronic packaging. This glass-metal composite may find some structural uses.

## 1.1 References

1. A.G.H.Dietz, 'Composite materials', 1965 Edger Marburg Lecture, American Society of Testing and Materials, Philadelphia, Pa.. 1965.
2. A. Mortensen and S. Suresh, *Intrn. Mater. Rev.*, Vol.40, No.6, 1995, p.239-265.
3. A.G.H.Dietz, 'Composite Engineering Laminates', MIT Press, Cambridge, Massachusetts, 1969.
4. C.S.Smith, 'A History of Metallography', University of Chicago Press, Chicago, Illinois, 1960.
5. G.D.Bengough, 'A study of the properties of alloys at high temperatures', *J.Inst.Metals*, 7(1912), p.123-174.
6. S.Hori, M.Tokizane and N.Furushiro, *Superplasticity in Advanced Materials*, The Japan Society of Research on Superplasticity, Osaka, Japan, 1991.
7. H.C.Tsai, K.Higashi and O.D.Sherby, 'Superplasticity in an Ultrahigh carbon Steel-Aluminum Bronze laminated Composite', *Advanced Composite'93*, International Conference on Advanced Composite Materials, Edited by T.Chandra and A.K.Dhingra, The Minerals, Metals & Materials Society, 1993, p.1287-1293. (Private Communication)

# Chapter 2

## Literature Review

### 2.1 Introduction

The word 'composite' means 'not consisting of a single part, rather of two or more distinct parts'. Thus a material having two or more distinct constituent materials or phases may be considered a composite material. It is only when the constituent phases have significantly different properties and thus the composite properties are noticeably different from the constituent properties that we come to recognize these materials as composite. The concept of composite materials is not new but it exists from the very prehistoric times[1]. The research of composite materials generated profound impact on science and technology as other major developments in the history of materials engineering because these materials have emerged as new structural materials with a broad range of engineering applications due to their unique capabilities of tailoring in performance and design. The spectrum of composite materials is uncomparably large since composite materials utilise polymeric, metallic or ceramic materials as their constituents in different form, in different volume percentage, and in different textural designs. Among all these, laminated composite material is a variety which consists of two or more layers or laminae (a single layer or plie of a laminate is called a lamina) of different materials completely bonded to each other so as to yield a composite material having properties different from and more desirable than those of its constituents. The laminated composite is having 'sharp' interface, not like diffused interface in functionally gradient materials[2]. By careful selection of layers, laminated composite materials provide a means for tailoring a composite to desired properties may be one or more of the following[3]:

- |  |   |                  |
|--|---|------------------|
| 1. corrosion resistance                    | 2. surface hardness   | 3. formability   |
| 4. wear resistance                         | 5. impact resistance  | 6. flexibility   |
| 7. toughness                               | 8. strength   | 9. appearance    |
| 10. improved heat transfer characteristics | 11. improved electrical properties  | 12. availability |
| 13. improved magnetic properties           | 14. controlled deformation(thermal expansion) in response to temperature change | 15. lower cost   |

For example, cupronickel cladding on copper provides a corrosion-resistant, low cost attractive appearance to coinage; and the difference in thermal expansion of the two metals in thermostat provides a controlled, reproducible deformation in response to temperature change.

## 2.2 Laminated Composite Fabrication methods

Laminated composites can be made by many techniques, which may be categorised roughly into three groups : bonding, deposition and spray forming. Bonding techniques start with component materials in sheet or plate form that are solid state bonded at the interfaces. In the case of deposition techniques, layers of component materials are formed sequentially by atomic or molecular scale transport of the component materials. Spray forming techniques, on the other hand, involve direct deposition of molten materials of the component materials into a laminate form. Details of these processing techniques, especially for commercial scale laminated composites, are mostly proprietary in nature. A technique is chosen depending upon the nature of materials, design of the component which is to be made with the material, where the component will be used.

### 2.2.1 Bonded laminates

Bonding techniques may be classified into several subgroups such as, adhesive bonding, melt-bonding, infiltration, diffusion bonding, reaction bonding, and deformation bonding. Surface preparation of the component materials, bonding temperature and pressure, interdiffusion and chemical reactions between the component materials greatly influence the microstructure, chemistry and bond strength at the interfaces and overall physical and mechanical properties of the resulting laminates.

### 2.2.1.1 Adhesive Bonding

Early versions of aluminium-laminates[4.5] were bonded with epoxy adhesives which resulted in an extremely high interfacial bond strength. The bonds could be made so strong that the laminates did not delaminate when pulled to failure. The laminates of mild steels with different interfacial bond shear strength (28 and 117  $\text{MNm}^{-2}$  respectively) were made using 'soft'(60Sn-40Pb) and 'silver'(61Ag-28Cu-11Zn) solders[6].

### 2.2.1.2 Melt-Bonding

Multilayer laminates of plain carbon steel and zinc can be made by dipping the steel sheets in the molten zinc and pressing them together during withdrawal[7]. This process is called melt bonding. The molten zinc between the sheets acted as a glue and solidified to form zinc/steel laminates.

### 2.2.1.3 Infiltration

Layers of aluminium are sandwiched between boron carbide tape and then heated to above the melting temperature of aluminium with subsequent infiltration. A different approach can be used, in which partial infiltration of nickel in the solid state into alumina was achieved. Nickel in sheet form and alumina as a tape cast sheet were stacked together and a high pressure was applied(1275MPa) for 3h at 1425°C. The product was a laminate containing alternating layers of alumina and nickel[2].

### 2.2.1.4 Diffusion Bonding

It is the solid state joining process in which two clean surfaces of similar or dissimilar materials are brought into contact usually at elevated temperature(temperature used is in the range of 0.5 to 0.8 times the melting or softening point of lower melting point species[8]) and with force applied normal to the bond plane and allowed to join together. The pressure applied is less than that required for largescale plastic flow[9].



### 2.2.1.5 Vacuum Hot Pressing

It is one of the most important techniques of diffusion bonding used for metals (e.g. aluminium, titanium), ceramics (e.g. silicon carbide) and also for composites (with matrix of Al, Cu, Mg, Ti, Ni). It is possible to have good control over the fabrication parameters in vacuum hot pressing. In addition, it can be quick, reproducible, and yield high-quality materials. But large pieces are difficult to consolidate by this process. An increasingly popular alternative of VHP is Hot Isostatic Pressing (HIP). In a HIP cycle, fluid pressure isostatically pushing against the HIPping canister acts to consolidate the piece. With HIP it is relatively easy to apply high pressure at high temperature over variable geometries. Step Pressing is a variation of the standard vacuum hot pressing technique. It involves performing repeated VHP cycles moving or stepping, the bagged lay up in the platens after each cycle. By step pressing parts which are larger than the hot-press platen size can be fabricated.

### 2.2.1.6 Reaction Bonding

Alternating thin foils of aluminium and nickel are stacked and then heated them to  $600^{\circ}\text{C}$  while applying a pressure of 10 MPa. The aluminium and nickel reacted to form an intermetallic NiAl phase at the aluminium and nickel interface. By adjusting the relative thickness of the foils, multilayer laminates of Al/NiAl or Ni/NiAl were made. Similarly,  $\text{Mg}/\text{Mg}_2\text{Al}_3$  or  $\text{Al}/\text{Mg}_2\text{Al}_3$  laminate can be made[2].

### 2.2.1.7 Deformation bonding

In deformation bonding, layers of the component materials are stacked and subjected to large plastic deformation until they are bonded together. Deformation bonding is the most efficient bonding technique from the industrial processing viewpoint and it includes press bonding, roll bonding, explosive bonding, hot-die molding, superplastic forming and diffusion bonding, hot drawing, co-extrusion[3,10]. Some of the processes are used for making laminates in plate or sheet form, and hot drawing and co-extrusion are used for making rod shaped laminates. Complex shapes can be made by hot-die molding and SPF/DB. In deformation bonding the plastic flow helps promote a strong bond between the components of the laminates by (a) placing the individual components of the laminate into close contact and (b) breaking oxide films and impurity layers that may interfere with the bonding process.

## 2.2.1.8 Press Bonding

The processing of laminates using press bonding requires careful selection of the temperature and strain rate of deformation. The deformation behaviour of a laminate during processing can be understood from the strain rate-stress behaviour of the individual components as shown in Figure 2.1. The plot in the Figure 2.1(a) shows a system in which compo-

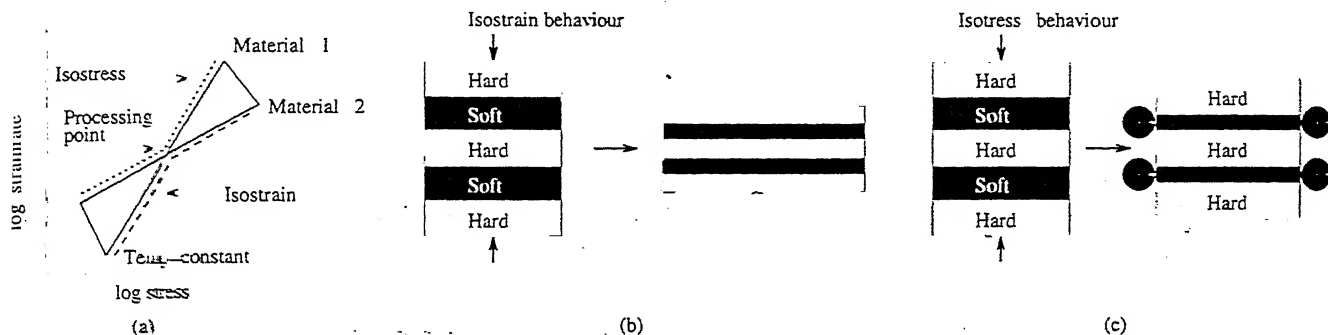


Figure 2.1: Deformation response of laminates during press bonding (a) strainrate-stress response; (b) isostrain behaviour; (c) isostress behaviour

nent materials have distinctly different strain rate- stress behaviour. The strain rate-stress response for the laminate is defined by the dotted area within the curves for the individual components. The upper bound for the flow stress of the laminate at a given strain rate is defined by Isostrain Behaviour, Figure 2.1(b) in which each component of the laminate undergoes the same strain. In practice, isostrain behaviour is approached when individual component layers are thin and frictional constraint or bonding between layers enforces uniform deformation. The lower bound for the flow stress of the laminate at a given strain rate is defined by Isostress Behaviour, Figure 2.1(c) in which each component is subjected to the same stress. Isostress behaviour requires the individual layers to act independantly and thus this type of behaviour is approached for thick layer systems. The ideal strain rate and temperature for the processing are chosen so that the components of the laminate have comparable flow stress which limits the extent to which one component can preferentially extrude from the laminate during processing. In practice, for thin layered systems there is considerable lattitude in the selection of temperature and strain rate for processing because frictional forces tend to enforce uniform deformation and a tendency to isostrain behaviour. Press bonding has been performed at  $750^{\circ}\text{C}$  for UHCS/brass laminates[11].

### 2.2.1.9 Roll Bonding

A semicontinuous technique which can be used for making laminate is roll bonding. Roll-bonding has been used to fabricate laminates of metals[3], wire-reinforced aluminium[12], UHCS/interstitial free iron[13], titanium[12], super-alloys[3]. Rolling can produce unidirectional monolayers or unidirectional or cross-ply composite laminates.

### 2.2.1.10 Hot Drawing and Co-extrusion

Hot drawing is another semicontinuous consolidation technique which has been developed for constant cross-section, unidirectional laminates. Fibre-reinforced wires produced by liquid infiltration can be used as precursors, canned in an inconel tube to form a billet. Muller et. al.[14] wound thin strips of Cu and Pd foils into a coil, encapsulated it in a thin walled can and then indirectly extruded it along the axial direction of the coil to obtain a multilayer lamellar structure.

## 2.2.2 Deposited Laminates

Deposition techniques involve atomic or molecular scale transport of the component materials such as in sputtering, evaporation, chemical or physical vapour deposition (CVD or PVD), or electroplating. With the exception of plating techniques, many of the deposition techniques are too slow and costly to be practical for making large scale, load bearing components. Several hundred micrometres thick laminates containing Cu and Monal layers with individual layer thickness of a few nanometres can be made using sputtering technique[15]. Electrodeposition technique can be used to make a  $50\mu$  thick laminate consisted of Ni and Cu layers with thickness ratio of 9:1 for Ni and Cu[16]. The magnetron vapour sputter deposition technique was used to produce  $Nb_3Al/Nb$  and  $Cr_2Nb/Nb(Cr)$  multilayer laminates with an average layer thickness of 2 and  $6\mu$ , respectively[17].

### 2.2.3 Spray Formed Laminates

Wu et. al.[18] spray deposited a multilayer laminate of 6061 and 6061-SiC, with a global SiC volume fraction of 15%, by periodically injecting SiC particulate into the atomised spray of the liquid Al 6061. The distribution of SiC particulates changed periodically

along the spray deposition direction, and discrete interface did not exit as is the case of the laminates made by pressing component material sheets together. This technique seems to be an attractive processing method, since it can create a layered structure directly from an aluminium alloy matrix and SiC powders.

## 2.3 Properties of laminates

### 2.3.1 General Constitutive Equation

The use of a laminate in any engineering application is advantageous only if it offers improvement in some property or combination of properties at a cost lower than that of a monolithic structure. So mathematical formulation of laminate properties from the properties of individual components is important. Conventional engineering materials can be described by only two terms : homogeneous and isotropic. Homogeneous means uniform, i.e. the material properties are not a function of position in the material and the word isotropic indicates that the material properties at a point in the body are not a function of orientation i.e all planes passing through a point in the material are planes of material property symmetry. In contrast, a laminated composite can be described by any of the following terms : homogeneous orthotropic; homogeneous anisotropic; heterogeneous orthotropic; heterogeneous anisotropic and quasi-isotropic. In an orthotropic material, only three mutually perpendicular planes of material property symmetry may be passed through a point. For an anisotropic material, there is no plane of material property symmetry which passes through a point. The term quasi-isotropic is used to describe a particular type of laminate that has essentially isotropic stiffness and perhaps strength. The simplest example is a 3-ply laminate with a  $0, \pm 60$  orientation. Of course, the more plies in the laminate, the less is the angle between the principle axes of each lamina; hence the laminate will better simulate an isotropic condition[19].

The elastic behaviour of a laminated composite under uniaxial loading within the plane of the composite, i.e. in any direction parallel to the laminae, is analogous to that of a uniaxial fibre-reinforced composite stressed to the fibre direction[3]. The anisotropy in a laminated composite can be effectively controlled, specifically in the case of fibrous composite. In case of unidirectional composite(UDC), the longitudinal strength is different from transverse strength, since the longitudinal properties are controlled by fibre properties while transverse properties are mainly controlled by matrix. This limitation is overcome in the case of orthotropic laminated composite or off-axis (quasi- isotropic) laminated composite.

Like elementary materials, a laminated composite can have a Hooke's law relationship that can be classified anywhere from homogeneous isotropic to heterogeneous anisotropic. And elastic symmetries and numbers of independent elastic constants describe the behaviour of isotropic, orthotropic and anisotropic materials. An orthotropic layer in a state of plane

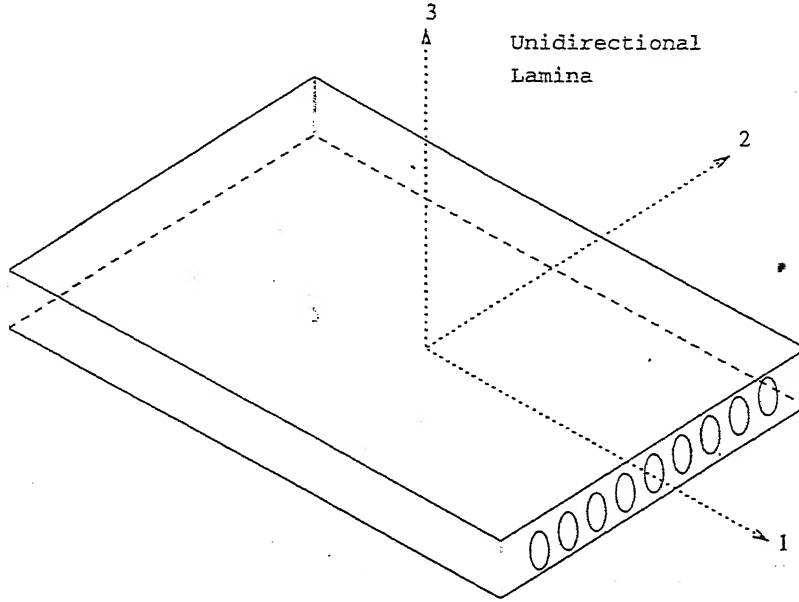


Figure 2.2: Lamina principal axis

stress may be characterized by the following relationship :

$$\begin{pmatrix} \sigma_1 \\ \sigma_2 \\ \tau_{12} \end{pmatrix} = \begin{pmatrix} Q_{11} & Q_{12} & 0 \\ Q_{12} & Q_{22} & 0 \\ 0 & 0 & Q_{66} \end{pmatrix} \begin{pmatrix} \epsilon_1 \\ \epsilon_2 \\ \gamma_{12} \end{pmatrix}$$

where the strains  $\sigma_1, \sigma_2, \tau_{12}$  and strains  $\epsilon_1, \epsilon_2, \gamma_{12}$  are referred to the 1-2-3 coordinate system - the principle or specially orthotropic co-ordinate system [Figure 2.2]. The components of the stiffness matrix,  $Q$ , are :

$$\begin{aligned} Q_{11} &= \frac{E_{11}}{1 - \nu_{12}\nu_{21}} \\ Q_{22} &= \frac{E_{22}}{1 - \nu_{21}\nu_{12}} \\ Q_{12} &= \frac{\nu_{21}E_{11}}{1 - \nu_{12}\nu_{21}} = \frac{\nu_{12}E_{22}}{1 - \nu_{21}\nu_{12}} \\ Q_{66} &= G_{12} \\ Q_{16} &= Q_{26} = 0 \end{aligned}$$

Transforming the above equation in any other axis system  $x-y-z$  and considering same deformation [Figure 2.3 ], the stress state in the  $k$ th ply can be written in terms of the midplane

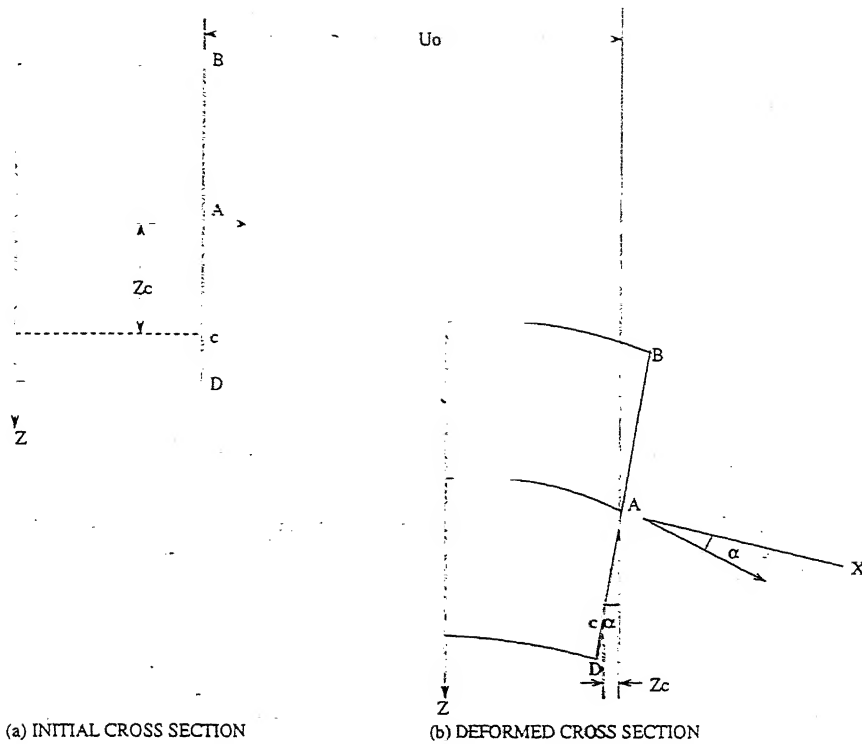


Figure 2.3: Bending geometry in the x-z plane (a) initial cross section; (b) deformed cross section

strains, the plate curvatures, the z coordinate and the plate elastic(stiffness) properties :

$$\begin{pmatrix} \sigma_x \\ \sigma_y \\ \tau_{xy} \end{pmatrix}_k = \begin{pmatrix} \bar{Q}_{11} & \bar{Q}_{12} & \bar{Q}_{16} \\ \bar{Q}_{12} & \bar{Q}_{22} & \bar{Q}_{26} \\ \bar{Q}_{16} & \bar{Q}_{26} & \bar{Q}_{66} \end{pmatrix}_k \begin{pmatrix} \epsilon^o_x \\ \epsilon^o_y \\ \gamma^o_{xy} \end{pmatrix} + z \begin{pmatrix} \bar{Q}_{11} & \bar{Q}_{12} & \bar{Q}_{16} \\ \bar{Q}_{12} & \bar{Q}_{22} & \bar{Q}_{26} \\ \bar{Q}_{16} & \bar{Q}_{26} & \bar{Q}_{66} \end{pmatrix}_k \begin{pmatrix} k_x \\ k_y \\ k_{xy} \end{pmatrix}$$

$$\left( \sigma \right)_k = \left( \bar{Q} \right)_k \left( \epsilon^o \right) + z \left( \bar{Q} \right)_k \left( k \right)$$

This expression can be used to complete the stress in a lamina when the laminate midplane strains and curvatures are known. In order to find a system of forces and moments acting at the geometric mid plane that is equivalent to the effect of these stresses, three stress resultants are defined which are equal to the sum or integral of these stresses in the z direction :

$$N_x = \int_{-\frac{h}{2}}^{\frac{h}{2}} \sigma_x dz$$

$$N_y = \int_{-\frac{h}{2}}^{\frac{h}{2}} \sigma_y dz$$

$$N_{xy} = \int_{-\frac{h}{2}}^{\frac{h}{2}} \tau_{xy} dz$$

The resultant of the stresses is not given entirely by the equivalent total loads. In addition, the moments must be applied at the midplane which are statically equivalent to the moments

created by the stresses with respect to this midplane. These moment resultants are given as :

$$M_x = \int_{-\frac{h}{2}}^{\frac{h}{2}} \sigma_x z dz$$

$$M_y = \int_{-\frac{h}{2}}^{\frac{h}{2}} \sigma_y z dz$$

$$M_{xy} = \int_{-\frac{h}{2}}^{\frac{h}{2}} \tau_{xy} z dz$$

The above force and moment equations define a system acting at the midplane of a laminate in terms of the laminate stresses. Q matrix expression defines the stresses acting on any layer or lamina in terms of the midplane strains (which are functions of the midplane displacements) and the plate curvatures (which are functions of the deflection  $w$ ). By combining these equations, the relationships between the force and moment system, the midplane strains, and the plate curvatures can be obtained. These relationships are the laminate constitutive equations. And, it is written as :

$$\begin{pmatrix} N \\ M \end{pmatrix} = \begin{pmatrix} A & B \\ B & D \end{pmatrix} \begin{pmatrix} \epsilon^0 \\ k \end{pmatrix}$$

where

$$A_{ij} = \sum_{k=1}^n (\bar{Q}_{ij})_k (h_k - h_{k-1})$$

$$B_{ij} = \frac{1}{2} \sum_{k=1}^n (\bar{Q}_{ij})_k (h_k^2 - h_{k-1}^2)$$

$$D_{ij} = \frac{1}{3} \sum_{k=1}^n (\bar{Q}_{ij})_k (h_k^3 - h_{k-1}^3)$$

## 2.3.2 Room Temperature Properties

### 2.3.2.1 Elasticity

The effective elastic modulus or specific stiffness (stiffness to density ratio) of a laminate depends not only on the elastic moduli, density, and volume fractions of the individual components comprising the laminate but also on their arrangement and the manner of loading of the laminated structure. It is assumed that each component of the laminate are isotropic in nature individually. The elastic behaviour of a laminated composite under uniaxial loading within the plane of the composite, i.e. in any direction parallel to the laminae, is analogous to that of a uniaxial fibre-reinforced composite stressed parallel to the fibre

direction. The density of the composite is given by  $\rho_c = \rho_1 V_1 + \rho_2 V_2$ ; where  $\rho_1$  and  $\rho_2$  are the densities of the components 1 and 2[20].  $V_1$  and  $V_2$  are the volume fractions respectively and given by  $V_1 = v_1/v_c$  and  $V_2 = v_2/v_c$ . Now assuming isostrain condition i.e. strains experienced by each components and composite itself are equal :  $\epsilon_1 = \epsilon_2 = \epsilon_3$  and considering sharing of load by each components we derive the following basic relationship :

$$\frac{\partial \sigma_c}{\partial \epsilon} = \frac{\partial \sigma_1}{\partial \epsilon} V_1 + \frac{\partial \sigma_2}{\partial \epsilon} V_2$$

. When both components deform elastically the basic relationship becomes  $E_c = E_1 V_1 + E_2 V_2$ . But when one of the components deforms elastically and another deforms plastically the basic relationship becomes

$$E_c = E_1 V_1 + \frac{\partial \sigma_2}{\partial \epsilon} V_2$$

. If both the components be ductile in nature, then during their simultaneous plastic de-

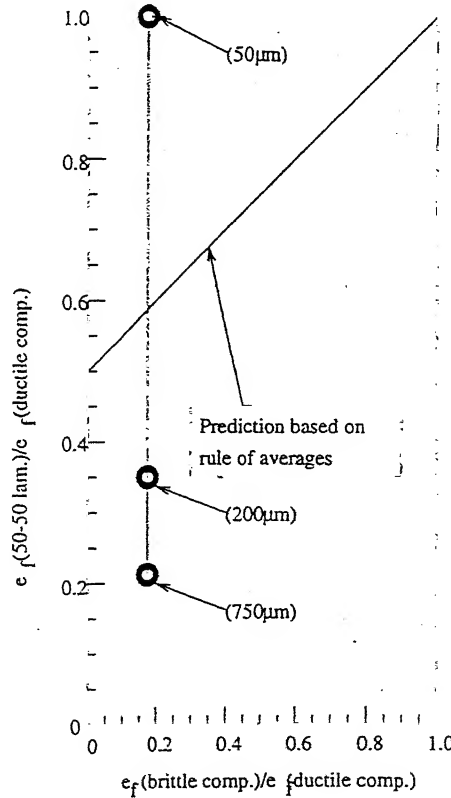


Figure 2.4: Experimental tensile elongation to fracture  $e_f$  of thick layer laminated UHCS/Brass composites containing 50vol% of each component compared with prediction based on rule-of-mixtures

formation, the laminate follows the basic relationship only. The fracture of the stronger component is followed by the failure of the composite[20]. Nevertheless, the tensile ductility of laminated composites cannot be predicted by the rule of averages. This is because the



tensile ductility of laminates is dependent on many variables, including the susceptibility of the less ductile layer to cracking, the contribution to cracking from the interlayer region, the ease of delamination and most importantly, the influence of layer thickness. The black rings in the above Figure 2.4 show the layer thickness effect. When the layer thickness is  $750\mu$ , tensile ductility is 13%, when layer thickness is  $200\mu$  tensile ductility is increased to 25%, and when layer thickness is  $50\mu$  tensile ductility is 60%[21].

Stiffness under bending loading within the plane of the composite can be calculated by rule-of-mixtures equations. In transverse bending or torsional loading, however, rule-of-mixtures behaviour is approximated for multiple-layered composites only if there is a large number of laminae and the distribution of high and low modulus materials is uniform across the thickness of the composite. In such a composite the stiffness of a rectangular beam or

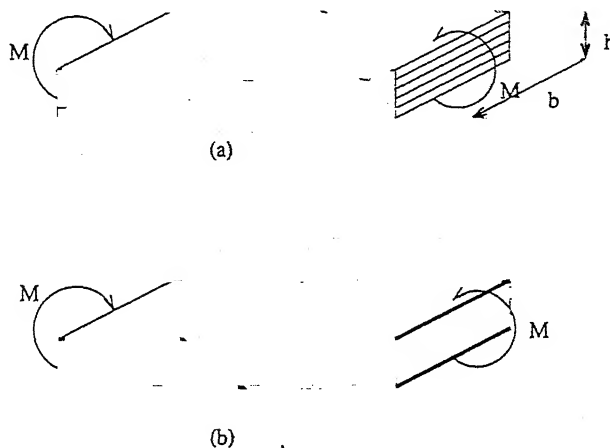


Figure 2.5: Schematic diagram of (a) uniform and (b) nonuniform laminates loaded in transverse bending

plate composed of many alternate layers of thin laminae of two materials, loaded as shown in Figure 2.5(a) would be similar to that of a homogeneous material :

$$M\left(\frac{1}{r}\right) = EI = E \frac{bh^3}{12}$$

where  $M$  is the applied bending moment,  $r$  the radius of curvature of the loaded beam, and  $b$  and  $h$  the base and height dimensions of the beam. The effective elastic modulus  $E$  is the same as the rule-of-mixtures modulus computed for uniaxial loading. If the distribution of the two materials is not uniform throughout the cross section (Figure 2.5(b)), the uniaxial rule-of-mixtures modulus cannot be used because stiffness in bending is determined predominantly by the outer layers, the contribution of each lamina being proportional to the square of its distance from the neutral axis. Stiffness of such a beam is given by

$$M\left(\frac{1}{r}\right) = \frac{b}{6} \int E x^2 dx$$

where  $x$  is the distance from the neutral axis. If the thicknesses of the laminae are small in comparison with the overall thickness of the composite, the stiffness of the laminate can be approximated by

$$M\left(\frac{1}{r}\right) = \frac{b}{12}(E_1 t_1 x_1^2 + E_2 t_2 x_2^2 + \dots + E_n t_n x_n^2)$$

where  $E_1, E_2, \dots, E_n$  are the Young's moduli of the individual laminae,  $t_1, t_2, \dots, t_n$  their thicknesses and  $x_1, x_2, \dots, x_n$  their distance from the neutral axis. Thus a small amount of high-modulus material can be applied to the outer surface of a low-modulus core to produce a laminate having relatively high stiffness in the bending mode[3].

### 2.3.2.2 Yield strength and Plasticity

Yielding under uniaxial tension occurs in one of the components of a laminated composite when the stress in that component exceeds its yield strength. In as much as the stress in each component is not necessarily the same as the average stress in the composite, it is more convenient to consider a critical *yield* strain criterion given by  $\epsilon_{y1} = \sigma_{y1}/E_1$  where  $\sigma_{y1}$  and  $E_1$  represent the yield strength and Young's modulus of the particular component of the laminate. Thus, yielding of a laminate occurs when the strain in the laminate exceeds the yield strain of any of the component laminae. Thus, the criterion for yielding is

$$\epsilon_c > \epsilon_{y1}, \epsilon_{y2}, \dots \text{or } \epsilon_{yn}$$

In terms of stress this criterion is

$$\frac{\sigma_c}{E_c} > \frac{\sigma_{y1}}{E_1}, \frac{\sigma_{y2}}{E_2}, \dots \text{or } \frac{\sigma_{yn}}{E_n}$$

It is interesting to note that in a hypothetical laminate consisting of steel ( $\sigma_y = 80 \times 10^3$  psi,  $E = 30 \times 10^6$  psi) and an aluminium alloy ( $\sigma_y = 30 \times 10^3$  psi,  $E = 10 \times 10^6$  psi), the stronger steel laminae would yield first. The predicted yield strength of such a composite laminate is thus given by

$$\sigma_{yc} = \frac{\sigma_{y*}}{E_*} E_c = \left(\frac{\sigma_{y*}}{E_*}\right)(E_1 f_1 + E_2 f_2 + \dots + E_n f_n)$$

where  $\sigma_{y*}$  and  $E_*$  are the yield strength and Young's modulus of the component laminae having the lowest  $\sigma_y/E_c$  ratio.[3]. Hawkins and Wright[22] found good agreement between their experimental results in the case of roll-bonded steel-copper composites and values predicted on the basis of the rule of mixtures using an equal-strain hypothesis. They also found that the plastic behaviour(i.e. the shape of the stress-strain curve after yielding) could also be predicted up to the point of plastic instability or necking in one of the components. It was found that the laminates followed the classical work-hardening equation,  $\sigma = K\epsilon^n$

and that the values of  $K$  and  $n$  could be synthesized either graphically from the stress-strain curves of the components using the equal-strain rule-of-mixtures approach or analytically from their individual work-hardening equations using the relationships

$$K = K_{Cu}t_{Cu} + K_{st}t_{st}$$

$$n = \log(\sigma_{Cu}t_{Cu} + \sigma_{st}t_{st}) - \log(K_{Cu}t_{Cu} + K_{st}t_{st})$$

where the subscripts Cu and st are used for copper and steel respectively to denote the coefficients, flow stress, and thickness. Hawkins and Wright also showed that drawing and stretch-forming stresses and punch loads can be predicted for two-layer and three-layer laminates. Qualitative predictions of drawability, formability, and earing tendencies could be made, but exact values of limiting draw ratios or Erickson values could not be calculated[3].

### 2.3.3 Thermal Expansion Co-efficient

Assuming each component of the laminate as isotropic in nature, the coefficient of thermal expansion can be given by,

$$\alpha_c = \frac{1}{E_c}(\alpha_1 E_1 V_1 + \alpha_2 E_2 V_2)$$

where  $\alpha_c$ ,  $\alpha_1$  and  $\alpha_2$  are coefficients of thermal expansion of composite, component 1 and component 2 respectively and  $E$  and  $V$  denote Young's modulus and volume fraction of components[20].

### 2.3.4 Fracture Toughness of laminated Ceramic composite with ductile reinforcements

For achieving high reliability structural ceramic materials having improved strength and toughness two different fundamental approaches viz. *flaw control* and *toughening* have carried out[23]. The former approach accepts the brittleness of the materials and attempts to create microstructures that impart sufficient fracture resistance. The toughening approach has the obvious advantage as the appreciable processing and post-processing damage can be tolerated without compromising the structural reliability. Reinforced ceramics have much greater strain-to-failure than that of their monolithic component. By virtue of different energy absorbing mechanisms i.e. toughening mechanisms the ceramic composites show pseudo-plasticity which results in non-linear elastic behaviour(Figure 2.6[23]). The fracture toughness and fracture energy value for different materials are given Table 2.1. The

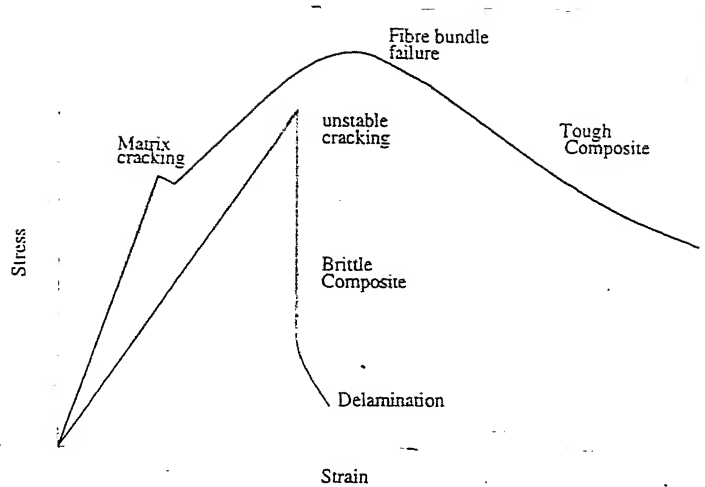


Figure 2.6: Schematic diagram illustrating the range of stress-strain characteristics exhibited by ceramic matrix composites

Table 2.1: Typical fracture energy and fracture toughness values for various materials[24]

Material	Fracture energy $G_c$ ( $kJm^{-2}$ )	Fracture Toughness $K_c$ ( $MPam^{1/2}$ )
<i>Polymers</i>		
epxy resins	0.1-0.3	0.3-0.5
Nylon 6.6	2-4	3
polypropylene	8	3
<i>Metals</i>		
pure Al	100-1000	100-350
Al alloy	8-30	23-45
mild steel	100	140
<i>Ceramics</i>		
soda glass	0.01	0.7
SiC	0.05	3
concrete	0.03	0.2
<i>Natural Materials</i>		
woods(crack grain)	8-20	11-13
woods(crack//grain)	0.5-2	0.5-1
bone	0.6-5	2-12
<i>Composites</i>		
fibreglass(glass/epoxy, planar random fibres)	40-100	42-60
Al-based particulate MMC	2-10	15-30
SiC laminate (crack layers)	5-8	45-55

different approaches to obtain improved toughness are following : microcracking, particle toughening by crack bowing, crack deflection at the particles and crack bridging by ductile particles, transformation toughening, matrix prestressing, reinforcement pullout, crack bridging by ductile reinforcements. Among these, ductile phase toughening is the most effective approach in ceramic-metal laminates. This is based on the ductile phase bridging of cracks in a ceramic environment. The bridging is associated with crack trapping or shielding and energy dissipation in the formation of a plastic zone and interface debonding[25]. As the crack extends in a ductile phase-reinforced ceramic composite, the toughening increase comes mainly from the amount of energy dissipated. Of course, the residual stresses, which are caused by thermal expansion mismatch, also are capable of suppressing crack propagation due to residual compressive stress field around the crack tip. For example, the increase in toughness due to ductile phase toughening with respect to monolithic  $Al_2O_3$  is easily apparent from Figure 2.7[25]. The high toughness of laminates, which is very important

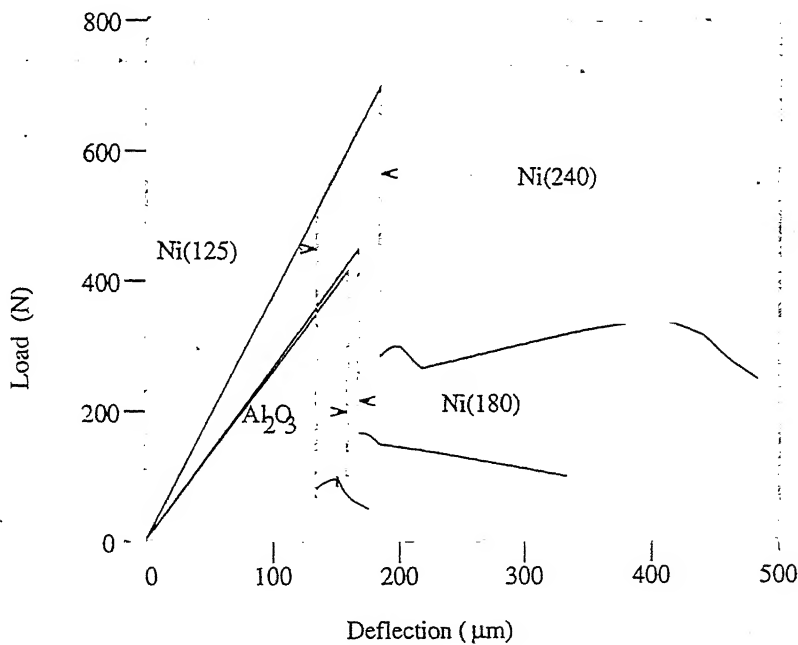


Figure 2.7: Load-deflection curves measured for flexure strength of laminates with different thicknesses of nickel layers and comparison with that of monolithic alumina

in practical terms, is closely linked with interfacial effects. A first step in exploring this is to analyse the conditions under which interfacial debonding i.e. crack propagation along an interface between two different materials, occurs. For a given loading configuration, the propagation of a crack along an interface between two constituents gives rise to an energy release rate,  $G_i$ , in much the same way as for the case when the crack is in a homogeneous material. Also, there is critical value,  $G_{ic}$ , an interfacial fracture energy, which  $G_i$  must

reach for the crack to propagate. Values of  $G_{ic}$  are not as readily available as  $G_c$  values for homogeneous materials. There are several reasons for this. Firstly, the toughness of an interface is sensitive to the way in which the interface was manufactured, rather than being unique to the pair of constituents on either side. A second reason is slightly more complex. Interfacial cracks often propagate under mixed mode loading conditions. This is in contrast to a crack in a homogeneous material, which will always tend to advance in a direction such that the stress field at the crack tip is purely tensile (mode I). An interfacial crack, however, is constrained to follow a predetermined path, depending on the loading configuration, the stress field at the crack tip may include a significant shear stress component acting on the plane of the interface (mode II). In general, the energy expended in debonding the interface is greater when there is a mode II component than for the case of pure mode I loading. This complicates the experimental measurement of  $G_{ic}$ . Not only can it be difficult to establish the exact stress field at the crack tip, it may vary with position in the specimen, particularly for reinforcement/matrix interfaces. The situation is further complicated if any residual stresses are present. The proportion of opening and shearing modes at the crack tip is often characterised by means of the phase angle,  $\psi$ . This is defined in terms of the mode I and mode II stress intensity factors, shown schematically in Figure 2.8[26].

One of the reasons for interest in interfacial toughness concerns crack deflec-

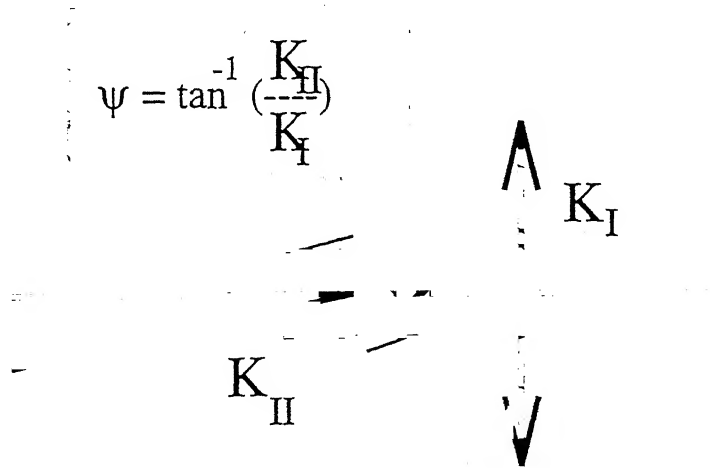


Figure 2.8: Schematic depiction of the stress field at an interfacial crack. The value of  $\psi$  can vary from  $0^\circ$  (pure mode I, crack opening) to  $90^\circ$  (pure mode II, shearing)

tion (Figure 2.9[26]). Thus critical issues of failure along a ceramic-metal interface involve knowing where a crack will initiate, the selected crack path, and the duration of crack growth and also interface chemistry and morphology, the loading type (cyclic vs. monotonic), the elastic properties of the metal and ceramic and the role of constrained plasticity[27]. Using mathematical modeling, some structure-performance maps of laminates, (similar to the con-

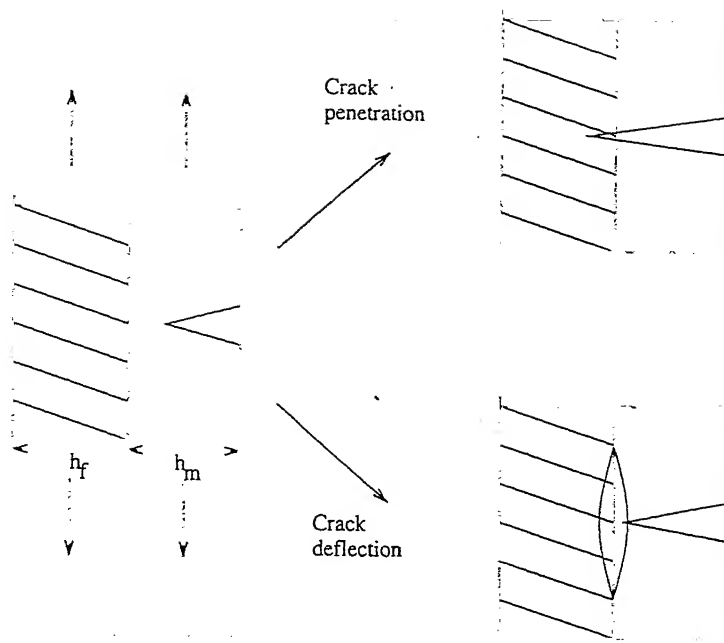


Figure 2.9: Geometry of crack deflection at an interface

cept of deformation maps by Ashby and the work of Dow[28,29]) can be drawn[30].

Lastly, one important factor controlling the performance of a ceramic laminate synthesized by tape casting, slip casting, centrifugal casting and dough rolling is the lamellar thickness because it controls the length of the crack propagation before interception of an interface[25]. Experiments indicate that a susceptibility to delamination cracking usually associates with a low transverse fracture resistance and a low interlaminar shear strength. Therefore, the presence and growth of delamination cracks in fibre-reinforced composites and composite laminates may tend to severe reliability and safety problems, such as the reduction of structural stiffness and exposure of the interior to an adverse environment which may cause the final failure. Safe performance of structural composite components then can only be assured through proper understanding of composite toughness and strength in light of the composite anisotropies[31]. In service, the loss of an electronic device from interface failure occurs more often by subcritical cracking in the bond, at applied stresses far below those required for catastrophic failure, from such mechanisms as thermal fatigue and environmentally induced crack extension. Crack growth behaviour along ceramic-metal interfaces must be regarded as a major in determining the reliability and long-term stability of these bonds[32]. It has been shown that the crack growth resistance in case of metallic glass-metal laminate composites is significantly greater than it is in monolithic form. Cracks grow catastrophically in monolithic glass but grow stably in a laminated composite. Crack tip shielding arising from bridging contributes most to this composite toughening. The bridging effect is a function of the properties of the metal in the laminate, since the bridging zone

size depends on such properties[33].

### 2.3.5 Glass-metal bonding and their interface

This subject is of great importance, because structural and electronic devices frequently require the combined use of ceramics and metals, and in many of these applications vacuum-tight seals are required. There are also the large industries of lamp manufacture, porcelain enamelling and ceramic-ware glazing, all dependent on the proper production of adherent interfaces between metal and glass or oxide ceramics. Indeed, the technological need for such combinations has been so great that development has occurred steadily despite incomplete understanding of the structural, chemical or mechanical nature of glass-to-metal interfaces.

The metals commonly used in making glass-metal seals are Pt, W, Mo, Cu, Ni, Fe and its alloys. Specific sealing glasses are needed for each metal and the pair has to be selected on the basis of specific properties and requirements. Most important requirement is a near match of thermal expansion coefficients, that is within 10%, with the metal having the larger coefficient. This matching assumes a greater importance as the bulk of glass increases, but does not appear to be critical in the formation of thin glass coating such as enamels. In case of porcelain enamel, the basic technology differs from glass-metal sealing because adherence is not dependent upon a proper pre-oxidation of metal surface, but on adherence-promoting oxides added to the glass composition.  $TiO_2$  or CoO are commonly used for this purpose. Sometimes, a transition layer of different material is used between glass and metal to overcome the problem of non-wetting of glass by metal. Glass and metal can be directly reaction welded with or without intermediate layer. Field-assisted bonding is another bonding technique that allows glass and metal to be bonded at temperature well below the softening point of the glass by applying a dc voltage in the range 20-500v across the substrate-glass couple so that the substrate metal is the anode and Pt in contact with the glass is the cathode.

The bonding of glass with metal can be explained by two theories :

1. mechanical theories : it is based on the development of a mechanical bond caused by the irregularities at the interface; dendritic theory(based on observations in some experiments of dendrites, irregular metallic growths of iron and cobalt, emanating from the glass towards the substrate metal) and electrolytic theory(a mechanism for substrate roughening based on electrolytic corrosion) come under this;
2. chemical theories : these stem from the requirement for  $O_2$  in making a bond and from the identification of an oxide at the interface of many bonds which show good adherence.



The above two theories say that the chemistry and structure of an interfacial layer is of paramount importance in controlling the effectiveness of glass- or ceramic-to-metal bonds. Theoretically, the strength of a bond can be analysed on the basis of the energy required to cleanly separate the glass and metal at the interface. Dr Duprè introduced the concept of work of adhesion and work of cohesion. The work of adhesion,  $W_{ad}$ , is equivalent to the change in energy on separating the glass from the substrate :  $W_{ad} = K(\gamma_v^s + \gamma_v^l - \gamma_l^s)$  where  $\gamma_v^s$  is the free energy of the solid-vapour interface,  $\gamma_v^l$  the free energy of the liquid-vapour interface,  $\gamma_l^s$  is a free energy of the solid-liquid interface and K is a constant. After cooling a glass-metal bond, both phases are solids, and so above equation must be modified to take account of the strain in the interface :  $W_{ad} = K(\gamma_v^s + \gamma_v^l - \gamma_l^s - \text{interfacial strain})$

Since interfacial strain is related to thermal expansion coefficient, above equation can again be modified to :  $W_{ad} = K(\gamma_v^s + \gamma_v^l - \gamma_l^s - f(\Delta\alpha)) \cdot A$

where A is the surface roughness which will affect the true contact area. Prior setting, the interface is formed from a liquid glass in contact with the metal and this concept gives rise to Young-Dupré equation :  $\gamma_v^s - \gamma_l^s = \gamma_g^l \cos\theta$

This Young's equation can be used to replace the interfacial energy term to give

$$W_{ad} = KA[\gamma_v^l(1 + \cos\theta) - f(\Delta\alpha)]$$

Thus for good bonding the requirements are[34] :

- a) the metal must have a large surface energy;
- b) the glass must have as large a surface tension as possible;
- c) the contact angle should be close to zero;
- d) thermal expansion mismatch between the components should not exceed 10%.

### 2.3.6 High temperature mechanical properties of laminates

The mechanical behaviour of laminated composites at elevated temperature has been principally studied for their potential superplastic behaviour. The studies have shown how a non-superplastic material can be made superplastic by lamination. The basis for this success is the achievement of a high strain rate sensitivity laminate by the appropriate choice of components. High strain rate sensitivity,  $m$ , inhibits neck formation and leads to high tensile ductility. Other laminate studies have involved the test to assess the stress state during compression deformation under testing perpendicular to the laminate direction. Such tests are useful as a guide to optimise open die forging or rolling of laminates. In another laminate study, elevated temperature creep properties were evaluated of a metal laminate system in

which interdiffusion occurs during high temperature exposure (Ni/Cu laminates). These studies are described in following subsections[2].

### 2.3.6.1 Constitutive relations for superplastic materials

The plastic flow stress of materials ( $\sigma$ ) is an instantaneous function of strain, strain rate and temperature i.e.  $\sigma = f(\epsilon, \dot{\epsilon}, T)$ . Considering constant strain for isothermal condition a general relation between flow stress and strain rate can be presented as

$$\sigma = C(\dot{\epsilon}^m)_{\epsilon, T}$$

at constant  $\epsilon$  and  $T$  where  $m$  is the strain rate sensitivity index which lies in the range 0.3 to 0.5 for superplastic materials. The exponent  $m$  can be obtained from the slope of a plot of  $\log \sigma$  vs.  $\log \dot{\epsilon}$ . However, a more sensitive way is a strain rate change test in which  $m$  is determined by measuring the change in flow stress brought about by a change in  $\dot{\epsilon}$  at a constant  $\epsilon$  and  $T$ ,

$$m = \left( \frac{\partial \ln \sigma}{\partial \ln \dot{\epsilon}} \right)_{\epsilon, T} = \frac{\dot{\epsilon}}{\sigma} \left( \frac{\partial \sigma}{\partial \dot{\epsilon}} \right)_{\epsilon, T} = \frac{\Delta \log \sigma}{\Delta \log \dot{\epsilon}} = \frac{\log \sigma_2 - \log \sigma_1}{\log \dot{\epsilon}_2 - \log \dot{\epsilon}_1}$$

Strain rate sensitivity of metals is quite low ( $< 0.1$ ) at room temperature but  $m$  increases with temperature, especially at temperature above half of the absolute melting point. In hot working condition  $m$  values of 0.1 to 0.2 are common[35]. But for other materials  $m$  is quite high. The extreme case is a Newtonian viscous solid, where flow can be described by  $\sigma = \eta(\dot{\epsilon})$ , where  $\eta$  is the apparent viscosity of the material. Large elongations result from the suppression of necking in the materials with high values of  $m$  and the extreme case is hot glass ( $m = 1$ ) which can be drawn from the melt into glass fibres without the fibres necking down.

### 2.3.6.2 Superplasticity in non-superplastic material by lamination

It is well known that single phase materials cannot be made inherently superplastic since a second phase is needed to stabilize the necessarily small grain size. This is unfortunate as the most corrosion resistant materials are generally single phase. But if such non-superplastic material is laminated with superplastic material then the laminate behaves like superplastic material. In this manner, high alloy material is conserved and high strength may be derived from the base material. As an added benefit, solid state bonding is enhanced

by the ultrafine superplastic microstructure, making possible unusually low cladding temperature. For superplasticity, the property of greatest traditional interest is the strain rate sensitivity index,  $m$ , given as,  $m = \Delta \ln \sigma / \Delta \ln \dot{\epsilon}$ , where  $\sigma$  is the flow stress at a strain rate  $\dot{\epsilon}$ . It has been shown that the experimentally obtained tensile elongation is strongly related to  $m$ . High tensile elongations are achieved when strain rate sensitivity is high. High strain rate sensitivity and superplasticity can be achieved in laminated composites based upon a superplastic component when tested in the laminate direction. This behaviour can be predicted by an isostrain model which states that the flow stress of the composite,  $\sigma_c$ , at a given temperature and strain rate is given by :  $\sigma_c = \sum f_i \sigma_i$ , where  $\sigma_i$  is the flow stress of component  $i$ , and  $f_i$  is the volume fraction of that component. The product  $f_i \sigma_i$  is simply the load necessary to deform the component  $i$  in a composite of unit cross section. By the isostrain model, the strain rate sensitivity exponent of a two component laminated composite may be related to the properties of its components by :

$$m_c = \frac{m_{sp} f_{sp} \sigma_{sp} + m_{nsp} f_{nsp} \sigma_{nsp}}{\sigma_c}$$

The subscripts  $c$ ,  $sp$ , and  $nsp$  relate the terms to the composite, the superplastic component, and the non-superplastic component, respectively. Thus, it is predicted that a laminated composite containing non-superplastic material may exhibit nearly ideal fine structure superplasticity provided the following conditions are met :

- a) the load necessary to deform the superplastic component is significantly greater than that for the non-superplastic component at the appropriate temperature and strain rate,
- b) the non-superplastic material is inherently ductile (i.e. the reduction of area at the failure is high)
- c) interdiffusion at the interface does not produce any harmful products which may impair superplasticity, and
- d) adhesion of laminate layers is sound.[36]

Considering iso-strain behaviour for analysis, one component is superplastic i.e a material whose deformation is controlled principally by grain boundary sliding (gbs) and the other component is non-superplastic material, i.e. a material whose deformation is controlled by slip (sl). A schematic diagram of the laminated composite and the testing direction, i.e. the isostrain orientation is illustrated in Figure 2.10(a). Because of the equal strain rates imposed on each of the two components, deformation of this composite requires that equal strain be imparted to each component. The deformation of such a composite can be described by an analogy consisting of two dashpots in parallel as shown in Figure 2.10(b). Each dashpot represents one of the components within the composite. This mechanical analogy demonstrates that the two dashpots are interlinked, that is the dashpots are forced

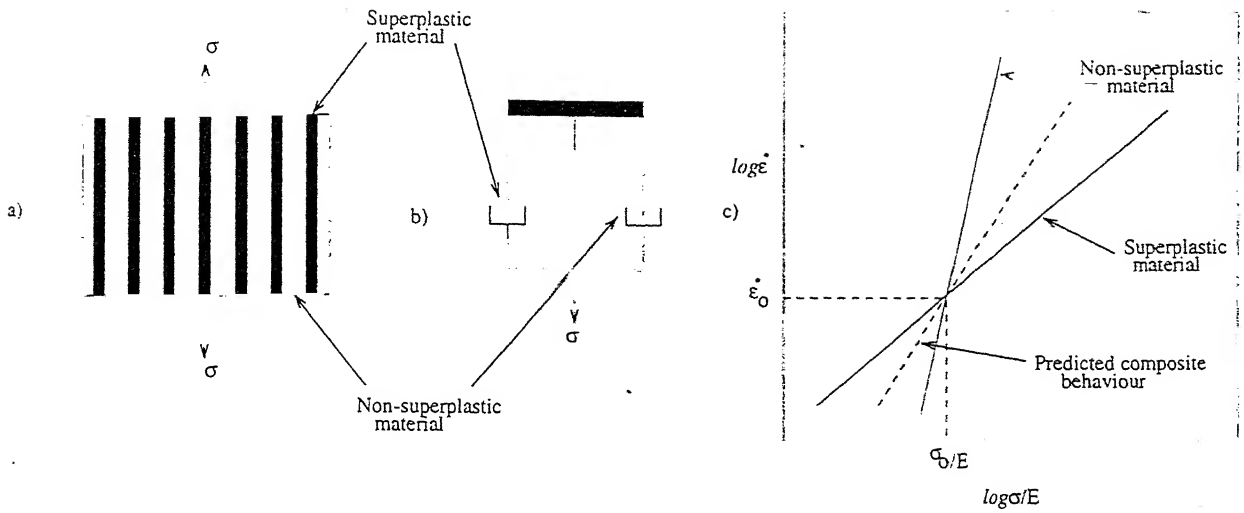


Figure 2.10: Schematic representations are shown in above figure of: (a) isotrastrain testing orientation of the laminated composites. (b) mechanical analogy of the deformation of a two-component composite; in the isotrastrain orientation the analogy consists of two dashpots arranged in parallel and subjected to a stress  $\sigma$ , (c) the predicted strain rate-stress behaviour of each of the two components as well as the overall behaviour of the laminated composite. As may be seen, the behaviour of the stronger of the two components.

to flow at the same rate under an imposed stress. The behaviour of the dashpots are therefore said to be interdependent. In this case of interdependent behaviour, the strongest dashpot controls the flow rate of the two-dashpot model. The deformation behaviour of each of the two components is shown in schematic form in Figure 2.10(c) as the solid lines on a plot of log strain rate ( $\dot{\epsilon}$ ) vs log flow stress ( $\sigma$ ). The predicted behaviour of a laminated composite, made from an equal volume fraction of each of the components, is shown in Figure 2.10(c) as the dashed line. At the high strain rate, the composite will be controlled by the superplastic component and therefore will have a high strain rate sensitivity index and is expected to be superplastic. At low strain rate, the composite will be controlled by the non-superplastic component, and therefore will have a low strain rate sensitivity index and is not expected to be superplastic. The equations for materials deforming by grain boundary sliding and slip may be written as follows :  $\sigma_{gbs} = K_{gbs} \dot{\epsilon}^{m_{gbs}}$  and  $\sigma_{sl} = K_{sl} \dot{\epsilon}^{m_{sl}}$ .

The method of determining the strain sensitivity index of a laminated composite containing these components will be illustrated as a) function of the imposed strain rate and b) a function of volume fraction of the superplastic component. Therefore, considering iso-strain behaviour from rule-of-mixture, we write

$$\sigma_c = f_{gbs} K_{gbs} \dot{\epsilon}^{m_{gbs}} + f_{sl} K_{sl} \dot{\epsilon}^{m_{sl}}$$

Table 2.2: Superplasticity in laminated composite

Material	Range of testing temperature K	$m_{c_{max}}$ obtd.	Range of $\dot{\epsilon}$ $s^{-1}$	$\epsilon_{max}$ %	Ref.
UHCS/I.F.iron	873-998	0.4	$10^{-6}$ - $10^{-2}$	430	13
SS-clad UHCS	1073-1123	0.45	$10^{-6}$ - $10^{-1}$	850	36
UHCS/Brass	983-1143	0.5	$10^{-5}$ - $10^{-1}$	60	37
UHCS/Bronze	1023-1123	0.5	$10^{-5}$ - $10^{-1}$	650	38
UHCS/mild steel	873-998	0.3	$10^{-4}$ - $10^{-2}$	70	39
Pure Al-clad	It remains superplastic, but no experimenal evidence given				40
Al-Cu-Zr					

The definition of the strain rate sensitivity index of the composite can be written for laminated composite as

$$m_c = \left( \frac{\partial \ln \sigma_c}{\partial \ln \dot{\epsilon}} \right)_{\epsilon, T} = \left( \frac{\dot{\epsilon}}{\sigma_c} \frac{\partial \sigma_c}{\partial \dot{\epsilon}} \right)_{\epsilon, T}$$

Now by substituting, we get

$$m_c = \frac{m_{gbs} f_{gbs} k_{gbs} \dot{\epsilon}^{m_{gbs}} + m_{sl} f_{sl} k_{sl} \dot{\epsilon}^{m_{sl}}}{f_{gbs} k_{gbs} \dot{\epsilon}^{m_{gbs}} + f_{sl} k_{sl} \dot{\epsilon}^{m_{sl}}}$$

The above equation can be modified to :

$$m_c = \frac{m_{gbs} + m_{sl} \left[ \frac{1}{f_{gbs}} - 1 \right] \left( \frac{k_{sl}}{k_{gbs}} \right) \dot{\epsilon}^{(m_{sl} - m_{gbs})}}{1 + \left[ \frac{1}{f_{gbs}} - 1 \right] \left( \frac{k_{sl}}{k_{gbs}} \right) \dot{\epsilon}^{(m_{sl} - m_{gbs})}}$$

Some practical examples of superplasticity in laminated composites are given in the Table 2.2 along with their experimental parameters. The activation energy for deformation of the laminated composite can be predicted analytically for an ideal case and it is given by [13]:

$$Q_c = \frac{f_{gbs} m_{gbs} Q_{gbs} \left( \frac{\sigma_{gbs}}{E} \right) + f_{sl} m_{sl} Q_{sl} \left( \frac{\sigma_{sl}}{E} \right)}{f_{gbs} m_{gbs} \left( \frac{\sigma_{gbs}}{E} \right) + f_{sl} m_{sl} \left( \frac{\sigma_{sl}}{E} \right)}$$

## 2.4 Characterization of laminated composites

The experimental characterization refers to the determination of the material properties through tests conducted on suitably designed specimens. The data obtained from the tests are appropriately reduced to evaluate various material properties that can later be used for analysis and design of practical structures. Understanding the material response over the entire range of loads is necessary if advanced design procedures are employed for

efficient material utilization. Elastic constants and strength are basic mechanical properties of materials. For a unidirectional lamina or composite, there are four independent elastic constants; the elastic moduli in the longitudinal and transverse directions; the shear

Table 2.3: Testing of laminate properties [41, 42, 43]

Test	Properties measured by the test
Uniaxial tension test	Elastic constants, strengths and strains in longitudinal and transverse direction, UTS, Poisson's ratio
Uniaxial compression test	Compressive strengths and strains in longitudinal and transverse direction
Shear tests	Shear modulus
(i) Short beam test	
(ii) Iosepescu test	
(iii) Lapshear test	
or double notch test	
Uniaxial bending test	Flexural Strength
(i) Three point bending	
(ii) Four point bending tests	
(i) Single-edge notched test	Fracture toughness
(ii) Double-edge notched test	
and (iii) notch bend test	
(i) Double cantilever beam (DCB) test (mode I)	Delamination failure
(ii) End notched flexure (ENF) test (mode II)	
(iii) Mixed mode bend (MMB) test	

modulus; the major Poisson's ratio and five independent strengths, namely, tensile and compressive strengths in the longitudinal and transverse directions and the in-plane shear strength. In the case of a laminate the interlaminar shear strength is also an important property. It is necessary to establish these properties for the minimum characterisation of a unidirectional lamina[21]. The testing of laminate properties are summarised in Table 2.3.

### 2.4.1 Testing of superplastic property

In practice, there are two different, but complementary, procedures for performing mechanical tests on superplastic materials. First, a series of tests may be conducted in which specimens are pulled on a machine which imposes a true or approximate constant strain rate. The steady-state flow stresses,  $\sigma$ , are then measured as a function of the imposed strain rates,  $\dot{\epsilon}$ , and the data are plotted logarithmically as  $\sigma$  vs.  $\dot{\epsilon}$ , as shown schematically on the left in Figure 2.11. Under these conditions, the stress and strain rate are related through the expression  $\sigma = B_1 \dot{\epsilon}^m$ , where  $B_1$  is a constant which includes the temperature dependence and  $m$  the strain rate sensitivity, represents the slope of the logarithmic plot. Data of this type generally tend to fall along a sigmoidal or three-stage type of curve, dividing the

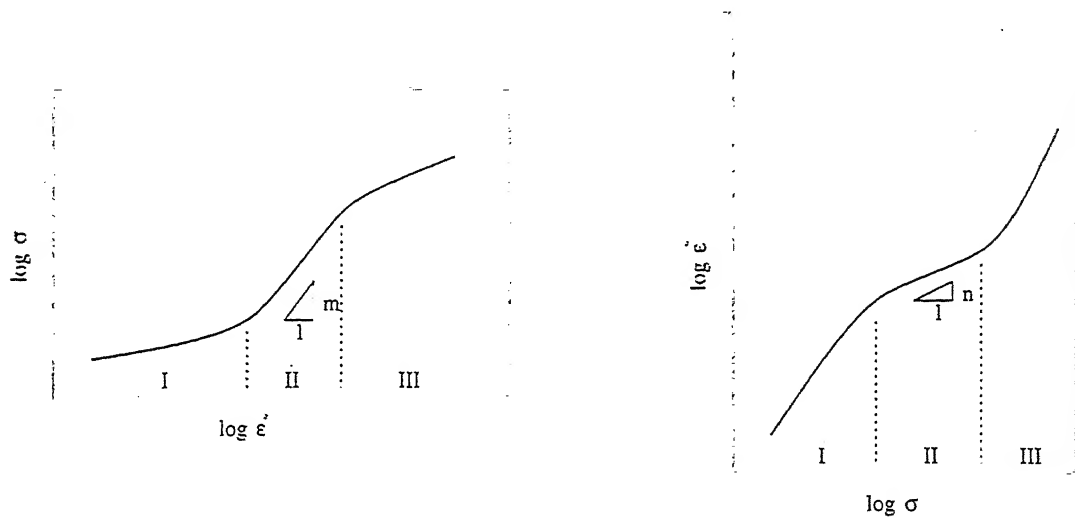


Figure 2.11: Schematic illustration of the two different procedures used to logarithmically plot the mechanical data of superplastic materials : stress vs. strain rate(left) and strain rate vs. stress(right)

behaviour into three distinct regions; region I at low strain rates where  $m$  is low, region II at intermediate strain rate where  $m$  is high and region III at high strain rate where  $m$  is again low. Second, superplastic specimens may be tested under creep conditions at a true or approximate constant stress. The steady-state strain-rates,  $\dot{\epsilon}$ , are then measured as a function of imposed stresses,  $\sigma$ , and the data are plotted logarithmically as  $\dot{\epsilon}$  vs.  $\sigma$ , as shown schematically on the right side of Figure 2.11. In this case the above eqn. is replaced by,  $\dot{\epsilon} = B_2 \sigma^n$ , where  $B_2$  is a constant and  $n$ , the stress exponent represents the slope of the logarithmic plot. The datum points obtained in this way again lie generally on a sigmoidal curve, with a low value of  $n$  in the intermediate region II and high values of  $n$  in regions I and III. Many examples of these two types of plots are available in the literature; and where

the two different experimental procedures have been conducted in the same investigation, the results are in excellent agreement[44].

The nature of bond can be reliably assessed by comparing the fracture characteristics of the bond with those of the parent material after a simulated bonding heat treatment. Ultrasonic evaluation of bond quality can be used but microvoids ( $d < 5\mu$ ) remain undetected. But interferometry method can be used for this purpose. Electron microscopy can be done to know the nature of bonding, new phase formation, interdiffusion of components and nature of fracture surface[9].

Table 2.4: Superplasticity in Al-alloys

Material	Temp. °C	$m$	$\dot{\epsilon}$ $s^{-1}$	$\epsilon$ %	Ref.
<i>Statically recrystallised</i>					
Al-33Cu	400-500	0.8	$8 \times 10^{-4}$	400-1000	45,46,47
Al-4.5Zn-4.5Ca	550	0.5	$8 \times 10^{-3}$	600	48
Al-(6-10)Zn-1.5Mg-0.2Zr	550	0.9	$1 \times 10^{-3}$	1500	
<i>Dynamically recrystallised</i>					
Al-6Cu-0.5Zr(SUPRAL 100)	470	0.3	$2 \times 10^{-3}$	1165	49
Al-6Cu-0.4Zr-0.3Mg-0.2Si-0.1Ge (SUPRAL 220)	460	0.65	$6 \times 10^{-4}$	1800	9
Al-4Cu-3Li-0.5Zr	450	0.5	$5 \times 10^{-3}$	900	50
Al-3Cu-2Li-1Mg-0.2Zr	500	0.4	$1.3 \times 10^{-3}$	878	
Al-5Mg-0.6Cu-0.7Mn-0.15Cr (NEOPRAL)	450-530	0.45-0.7	$1 \times 10^{-3}$	700	9
Al-6Mg-0.4Zr	520	0.6	$2 \times 10^{-4}$	885	51
Al-6Zn-3Mg	320-360	0.3	$10^{-3}$ - $10^{-2}$	200-400	52
Al-9Zn-1Mg-0.3Zr	550	0.9		1550	53
Al-5.5Zn-2.5Mg-1.5Cu-0.2Cr (7475)	515	0.5-0.8	$10^{-4}$ - $10^{-3}$	1200	54,55
Al-6.2Zn-2.5Mg-1.7Cu (7010)	520	0.65	$10^{-5}$	350	9
Al-2.5Li-1.2Cu-0.6Mg-0.1Zr (8090)	500-540	0.4-0.55	$10^{-4}$ - $10^{-3}$	500-1000	9
Al-3Li-0.5Zr	425-475	0.45	$10^{-3}$ - $10^{-1}$	500-1000	51



## 2.5 Individual properties

### 2.5.1 Superplasticity in aluminium alloys

A large number of aluminium alloys show superplastic behaviour at moderately high temperature. Some of them have achieved commercial importance. The superplastic properties of aluminium alloys are summarised in the following Table 2.4.

### 2.5.2 Zn-Al alloy system

Early work of Backofen and his group found that 80%Zn-20%Al(wt%) alloy shows maximum elongation(650%) at 250°C[56]. The superplastic property of Zn-22wt%Al eutectoid alloy is attributed by the ultrafine grain size ( $< 10\mu\text{m}$ ) produced by phase separation. If the alloy is quenched from above monotectoid temperature(375°C)(Figure 2.12) to room temperature a supersaturated solid solution of Al in Zn is formed which decomposes in a spinodal fashion producing a very fine grain, highly superplastic, microstructure[9]. Some established data about structural superplasticity of Zn-22%Al eutectoid is given in Table 2.5.

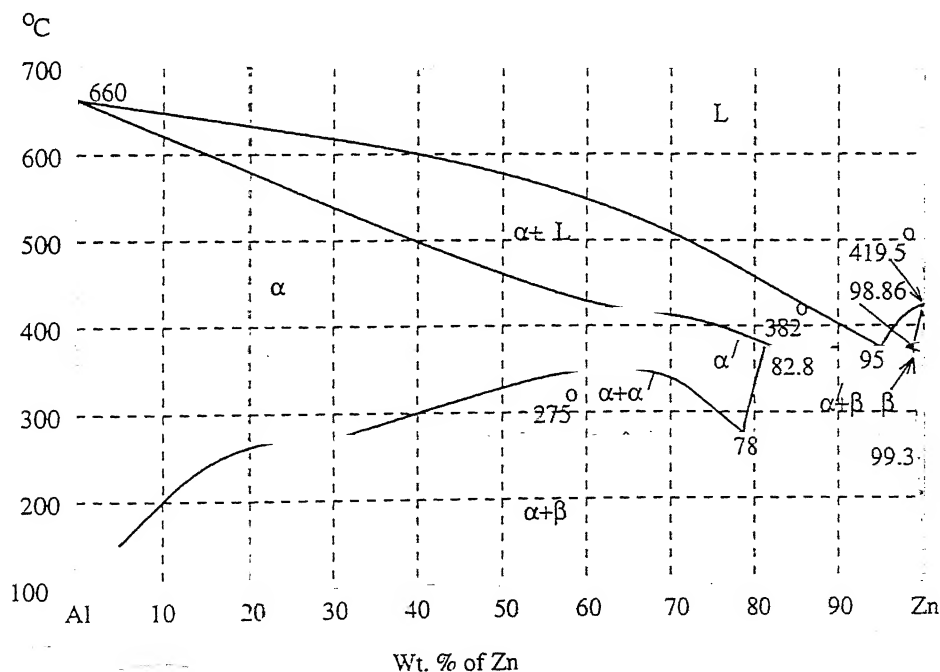


Figure 2.12: Schematic phase diagram of Zn-Al system

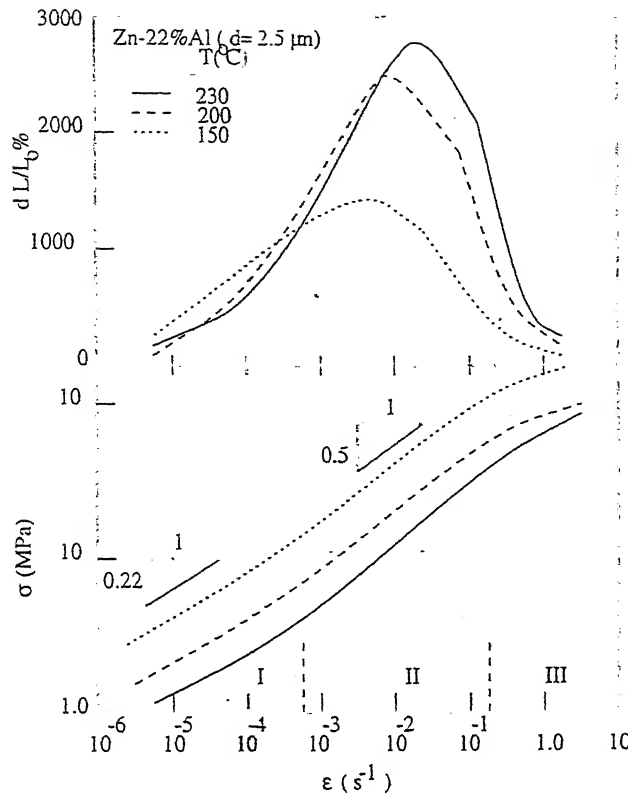


Figure 2.13: Elongation to failure(upper) and flow stress(lower) vs. initial strain rate for Zn-22%Al having a grain size of  $2.5\mu\text{m}$  tested in the temperature range from  $150^\circ\text{C}$  to  $230^\circ\text{C}$ .

In Zn-Al eutectoid alloy, the strain rate sensitivity in region I ( at low strain rate) is low and this has been interpreted as evidence for some form of threshold stress for superplastic flow since dislocation activity is not normally observed at such low strain rates. But some times it has been observed that at low strain rates strain rate sensitivity increases towards unity and this has been cited as evidence for diffusion controlled flow with the activation energy for flow in region I being similar to that measured for volume diffusion[9]. This is contrary to the expectation for fine grained material i.e. the activation energy would be that for grain boundary diffusion. Unlike the result shown in Langdon's review[44] (Figure 2.13) Nicholson[57] showed that the various stages in  $\log \sigma_t - \log \dot{\epsilon}_t$  plot are not well defined in Zn-Al eutectoid alloy and the stress-strainrate curves are essentially linear over a wide range of strain rates(Figure 2.14). For Zn-Al eutectoid system, the relation  $Q_{\dot{\epsilon}}/Q_{\sigma} = m$  is valid[58, 59, 60]. In Zn-Al alloys containing aluminium in the range 0.2 to 50 wt% structural

Table 2.5: Superplasticity in Zn-22Al alloy[61]

Maximum strain rate sensitivity index(m) :	0.7
Maximum % elongation :	2900
Temperature range :	20 – 300°C
Activation energy for superplastic deformation :	24.8 – 96.6 KJ/mol
	59.2
	64.7
	74.8 – 121.0
	88.2 – 148.3
	54.0 – 84.0
	73.0 – 119.7

superplasticity has been established. However, the superplastic characteristics became less pronounced on either side of the eutectoid composition. Although the flow stress and the temperature of maximum ductility increases with increasing Al-content in the alloy, while the strain rate consistent with maximum elongation decreases. Addition of Cu(upto 1%) or Mn to the Zn-Al eutectoid alloy leads to three stage flow stress- strain rate behaviour in the ternary alloy while in the binary alloy region I could not be detected[61]. In situ TEM[62,63] of thin foils of Zn-Al reveals (a) grain boundary sliding and grain rotation (b) no tangle/cell or void formation (c) no recrystallisation (d) negligible grain growth and integrity of interfaces (e) random switching of grains. In the case of this alloy when the initial structure is isotropic, the basal plane pole figures of the Zn-rich phase obtained from specimens deformed at optimal strain rates closely resemble those of the starting material. On the otherhand,

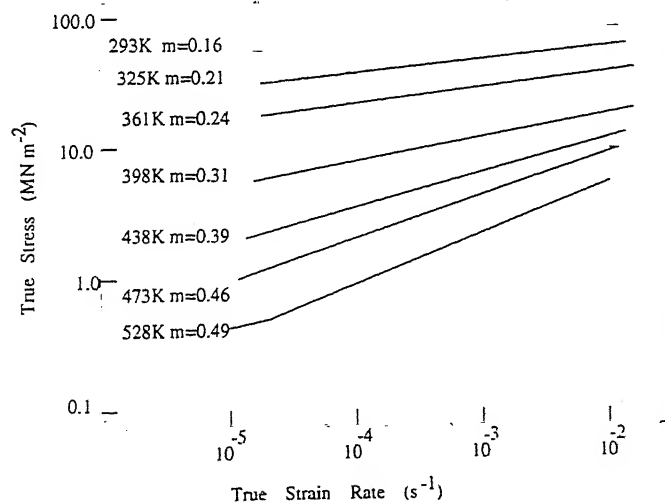


Figure 2.14: Linear variation of stress with strain rate in Zn-22Al eutectoid.

deformation at higher non-superplastic strain rates gives rise to sharply textured pole figures analogous to those seen in case of cold rolled zinc. This shows the uniformity of strain in region II[64].

### 2.5.3 Deformation of glass

At room temperature, glass behaves like an elastic solid whose deformation is time-independent and recoverable. It is brittle at lower temperature. But when temperature is increased the atomistic diffusion in glass increases and it becomes deformable. So glass becomes inelastic at higher temperature provided there is no crystallisation within it. The inelastic behaviour may be viscous or plastic depending on some physical parameters. In Figure 2.15 are summarised the lines from the deformation maps of polythene(a long-chain polymer), glass, alumina and diamond[65]. A small change in temperature tends to produce a large change in the stress needed to generate a flow rate of  $10^{-7} \text{ s}^{-1}$  in these non-metals. By contrast, the dependence of the flow stress in metals such as copper, aluminium and a strong alloy(Nimonic 105) is comparatively small[Figure 2.15] and McLean points out that it is the activation volume that can explain this difference, particularly the difference between glasses and metals. Thus temperature and stress dependence of the flow process is typically of form :

$$\dot{\epsilon} = A \exp \left[ - \frac{Q - V_a \sigma}{kT} \right]$$

where  $V_a$  is the activation volume and  $Q$  the activation energy for the flow process. The viscosity of glass is strongly dependent on temperature and it influences the deformation behaviour. The temperature-dependence of the viscosity of some glasses are shown in Figure 2.16[66].

## 2.6 Scope of this work

The purpose of this work is to study the simultaneous deformation behaviour of glass and metal. Above softening point(defined by viscosity of  $10^7 \text{ Pa s}$ ) glass starts to deform inelastically defying its elastic behaviour at lower temperature and higher viscosity. Around working point(defined by viscosity of  $10^3$  to  $10^4 \text{ Pa s}$ ) it deforms inelastically obeying the nature of ideal Newtonian fluid in case of which  $\sigma = \eta(\dot{\epsilon})$  holds. Glass is an isotropic solid random network structure solid without any grain or grain boundary. So it does not follow any mechanism applicable to solids, rather behaves like a fluid at higher temperature and

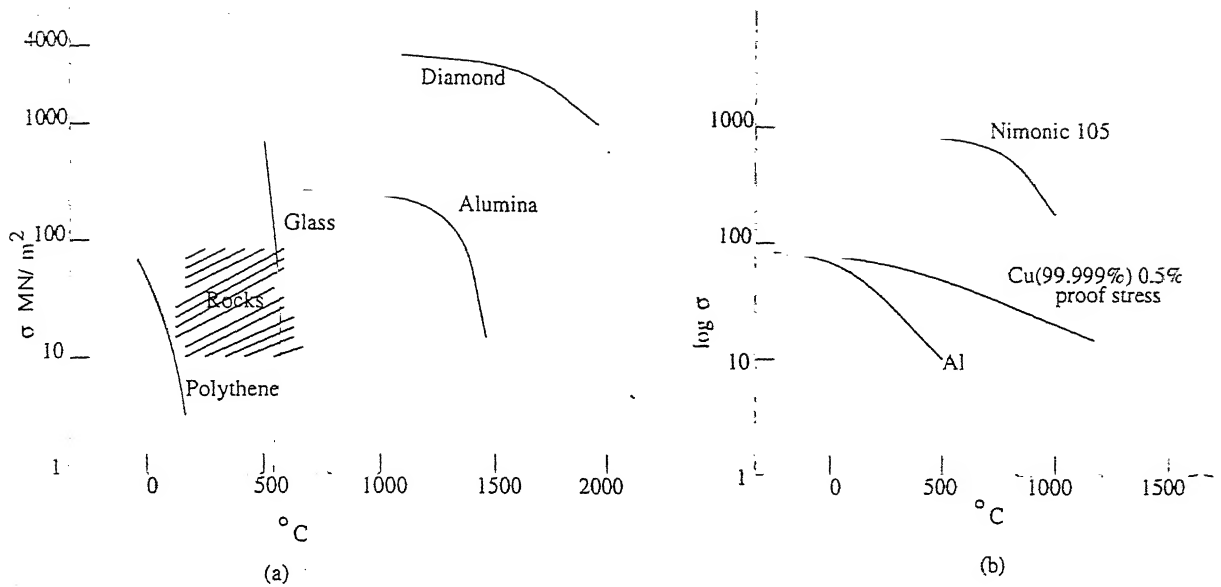


Figure 2.15: Lines from the deformation maps of some (a) non-metals and (b) metals for a deformation rate of  $10^{-7}/\text{sec}$ .

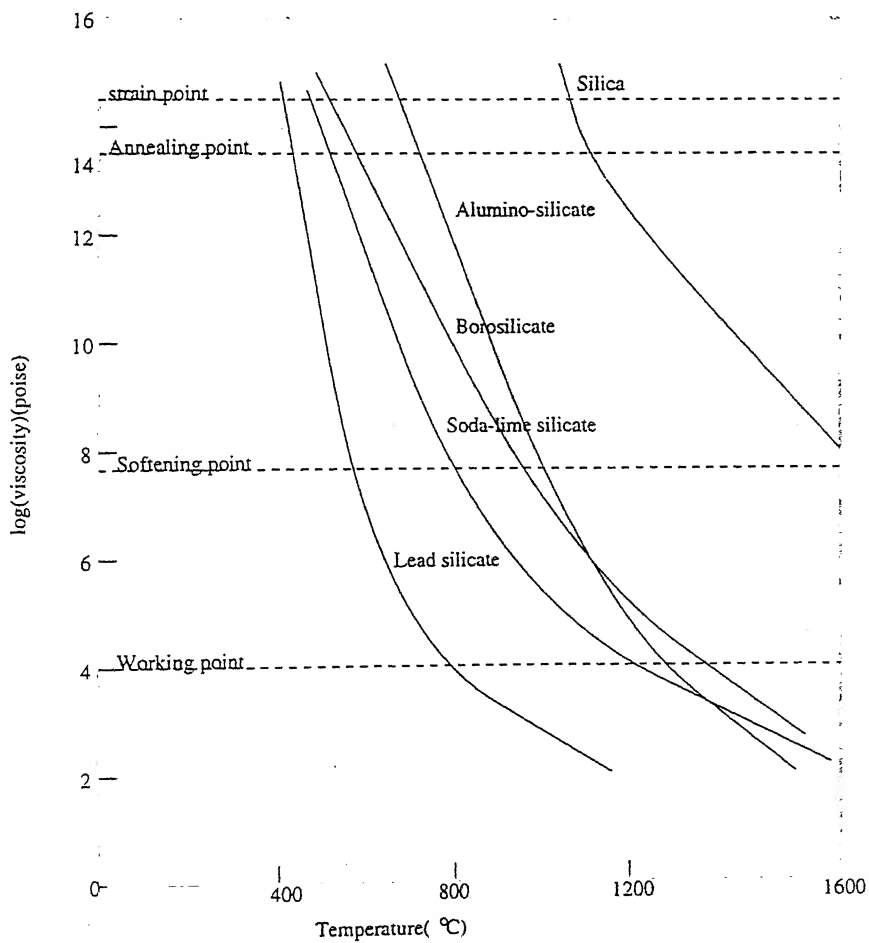


Figure 2.16: Variation with temperature of the viscosity of some commercial glasses

lower viscosity. On the other hand, metal is anisotropic in nature and deforms primarily by dislocation movements within and/or across grain boundary. At higher temperature, some metals deform primarily by grain boundary sliding rather than by slip. These metals are superplastic in nature and persistent to exceptionally high strains. In the present study, a glass (in powder form) is diffusion bonded to a superplastic alloy and they were tested at higher temperature to check which component of the laminate is dominant and governing the overall deformation process. To form a good glass/metal bond cautious selection of each component is required.

## 2.7 References

1. C.S. Smith, A History of Metallography, University of Chicago Press, Chicago, Illinois, 1960.
2. D.R. Lesuer, C.K. Syn, O.D. Sherby, J. Wadsworth, J.J. Lewandowski, and W.H. Hunt, Jr., Intl. Mater. Reviews, 1996, vol. 41, No. 5 p169
3. E.S. Wright and A.P. Levitt, "Laminated-Metal Composites", in Composite Materials, ed. L.J. Broutman and R. Krock, Vol. 4 "Metallic Matrix Composite", ed. K. Kreider. Academic Press, Inc., 111 Fifth Avenue, New York 10003, 1974
4. J.G. Kaufman, J. Basic Eng. (Trans. ASME), Sept. 1967, p. 503-507.
5. J.A. Alic and A. Danesh, Eng. Fract. Mech., 1978, p. 177-186.
6. J.D. Embury, N.J. Petch, A.E. Wraith and E.S. Wright, Trans. AIME, 239, 1967, p. 114-118.
7. A.J. Vazquez and J.J. Damborenea, Process. Adv. Mater, 1, 1991, p. 55-60.
8. B. Derby and E.R. Wallach, Metal Science, Vol. 18, 1984, p. 427.
9. J. Pilling and N. Ridley, 'Superplasticity in Crystalline Solids', The Institute of Metals, 1989.
10. R.K. Everett and R.J. Arsenault (ed.), "Metal Matrix Composite : Progress and Interfaces, Academic Press, 1991.
11. H.C. Tsai, J. Wolfenstine and O.D. Sherby, Composites, 22, 1991, p. 373-379.
12. J.J. Moore, D.V. Wilson and R.T. Roberts, Mater. Sci. Eng., Vol. 48, 1981, p. 113.

13. B.C.Synder, J.Wadsworth and O.D.Sherby. *Acta Metall.*, Vol.32, 1984, p.919-932.
14. K.Muller, D.Ruppin and D.Stockel, *Metall.*, Vol.39, 1985, p.26-33.
15. T.W.Berbee, Jr., in " Physics, Fabrication, and Application of multilayer structures", (ed. P.Dhez and C.Weisbuch), p.17-32, 1988, New York, Plenum Press
16. D.Tench and J.White, *Metall. Trans.*, 1984, Vol.15A, p.2039-2040.
17. R.G.Rowe, D.W.Skelly, M.Larsen, J.Heathcote, G.Lucas and G.r. Odette, in " High temperature silicides and refractory alloys", (ed. R.G.Rowe et.al.) p.461-472, 1994, Pittsburgh, PA, MRS.
18. M.Wu, J.J.Zhang, W.H.Hunt,Jr., J.J.LEwandowski and E.J.Lavernia, in " Processing and fabrication of advanced materials 4", (ed. J.J.Moore and T.S.Srivatsan), 1995, Warrendale, PA, TMS.
19. J.C.Halpin, "Primer on composite materials analysis", Technomic Publishing Co.Inc.
20. B.D. Agarwal and L.J. Broutman, "Analysis and performance of fiber composites John-Wiley & Sons, 1980.
21. C.K. Syn, D.R. Lesuer, J. Wolfestine and O.D. Sherby, *Metall. Trans.*, 1993, Vol.24A, p.1647-1653.
22. R. Hawkins and J.C. Wright, *J.Inst.Metals*, Vol.99, 1971, p.357-371.
23. A.G. Evans, *J. Am. Cer. Soc.*, 73[2], 1990, p.187-206.
24. M.F. Ashby and D.R.H. Jones, "Engineering Materials", Pergamon, Oxford, 1980.
25. Z. Chen and J. Mecholsky,Jr, *J.Am.Ceram.Soc.*, 76[5], 1993, p.1258-1264.
26. D. Hull and T.W. Clyne, "An Introduction To Composite materials", Cambridge University Press, 1996.
27. R.O. Ritchie, R.M. Cannon, B.J. Dalgleish, R.H. Dauskardt and J.M. McNaney, *Mater.Sci& Vol.A166*, 1993, p.221-235.
28. M.F. Ashby, C. Gandhi and D.M.R. Taplin, *Acta Metall*, Vol.27, 1979, p.699.
29. H.J. Frost and M.F. Ashby, "Deformation Maps", Pergamon Press, Oxford,U.K.,1982.
30. T.W. Chou and J.M. Yang, *Metall. Trans.*, Vol. 17A,No.9, 1986, p.1547-1559.

31. P.G. Charalambides, J.Am.Ceram.Soc., Vol.74, No.12, 1991. p.3066-3080.
32. T.S. Oh, R.M. Cannon and R.O. Ritchie, J.Am.Ceram.Soc., Vol.70, 1987, p.c352-c355.
33. Y. Lang and T.H. Courtney, Metall. Trans.. Vol.21A, No.8, 1990, p.2159-2167.
34. I.J. McCollm, "Ceramic Science for Materials technologists", Leonard Hill,1983.
35. G.E. Dieter, "Mechanical Metallurgy" , McGraw Hill.
36. G.S. Dahlen, D.W. Kum and O.D. Sherby, Metall. Trans., Vol.17A, 1986, p.2295-2298.
37. H.C. Tsai, J. Wolfenstine and O.D. Sherby, Composites, Vol.22. No.5, 1991, p.373-379.
38. H.C. Tsai, K.Higashi, and O.D. Sherby, "Advanced Composites '93(International Conference on Advanced Composite Materials)(ed. T.Chandra and A.K. Dhingra), TMS,1993.
39. G. Bhanuprakash Babu and R.K. Dubey, ISIJ International, Vol.xx, No. 11, 1996, p.1184-
40. R. Grimes, C. Baker, M.T. Stowell and B.M. Watts, Aluminium Vol. 51, 1975.
41. A.M. Borzdyka, "Elevated temperature testing of metals", Israel Program for Scientific Translation, Jerusalem, 1965.
42. L.A. Carlson and R.B. Pipes, "Experimental characterization of advanced composite materials", Technomic Publishing Co. Inc., 1997.
43. J. Harvey, P.G. Partridge and C.L. Snooke, J.Mater.Sci, Vol.20 1985, p.1009.
44. T.G. Langdon, Metall.Trans., 1982, Vol.13A, p.689-701.
45. D.L. Holt and W.A. Backofen, Trans ASM 59 , 1966, p.755-768.
46. K.A. Padmanabhan and G.J. Davies, Metal Sci, 11, 1977, p.177-184.
47. G. Rai and N.T. Grant, Metall. Trans, vol.6A, 1975, p.385-390.
48. D.M. Moore and L.R. Morris, Mater. Sci. and Eng., Vol.43, 1980, p.85-92.
49. R.H. Bricknell and A.P. Bentley, J.Mater.sci, Vol.14, 1979, p.2547-2554.
50. J. Wadsworth, Metall. Trans., Vol.16A, 1985, p.2312-2332.
51. K.Matsuki, Y.Uetani, M.Yamada and Y.Murakami, Metal Sci, Vol.10, 1976, p.235-242.



52. R.H.Bricknell and J.W.Edington. Metall. Trans, Vol.7A, 1976, p.153-155.
53. K.Matsuki, H. Morita, M. Yamada, and Y.Murakami, Metal Sci. Vol.11, 1977.p.156-163.
54. C.H. Hamilton, C.C.Bampton and N.E. Paton, "Superplastic forming of structural alloys", (ed. C.H. Hamilton and N.E. Paton). TMS-AIME, 1982, p.173-189.
55. C.C. Bampton, J.A. Wert and M.W. Mahoney, Metall. Trans., Vol.13A, 1982. p.193-198.
56. W.A.Backofen, I.R.Turner and D.H.Avery, Trans. Am. Soc. Met., Vol.57, 1964. p.980.
57. R.B.Nicholson, 'Electron Microscopy and the structure of materials, ed. G.Thomas, Berkeley, University of California Press , 1972, p.689.
58. K.A.Padmanabhan and G.J.Davies, Phys. Stat. Solidi (a) Vol.18, 1973, p.295.
59. M.D.C.Moles and G.J.Davies, Met.Sci. Vol.10, 1976, p.314.
60. P.Maulik and K.A.Padmanabhan, J.Mater.Sci. Vol.10, 1975, p.1646.
61. K.A.Padmanabhan and G.J.Davies, 'Superplasticity', Springer-Verlag, 1980.
62. H.Naziri, R.Pearce, M.H.Brown and K.F. Hale, J.Microscopy, Vol.97, 1973, p.229.
63. H.Naziri, R.Pearce, M.H.Brown and K.F. Hale, Acta Metall. Vol.23, 1975. p.489.
64. D.J.Lee, J.Inst.Met., Vol.99, 1971, p.66.
65. D. McLean, Trans. Met. Soc. AIME, Vol.242, 1968, p.1193-1203.
66. J. Gittus, "Creep, viscoelasticity and creep fracture in solids", Applied Science publishers Ltd. London, 1975.

# Chapter 3

## Experimental Details

### 3.1 Selection of materials

To make a strongly bonded glass-metal laminate the thermal expansion coefficients of the components should be such that the thermal expansion coefficient mismatch between them is small. Preferentially the thermal expansion coefficient of glass should be lower than that of metal to ensure a compressive residual stress in glass. Glass can tolerate more compressive stress compared to tensile stress. So for selection of components in a glass-metal laminate, the most important criterion is the matching of their thermal expansion coefficients. In the present study, the mismatch between their thermal expansion properties is very small. Second criterion is the temperature of deformation of the glass and the metal. The softening point of the glass should be in the temperature range of superplastic deformation of the metal. This property facilitates the high temperature simultaneous plastic deformation of glass and metal. The properties relevant to the present study are summarized in the following Table 3.1.

### 3.2 Preparation of metal strips

Rolled and recrystallised sheet of eutectoid zinc-aluminium was supplied. Zn-Al alloy pieces were cut from sheet and hot rolled at 250°C giving a reduction of 85 – 90%. The rolled sheets were annealed at 250°C for 10min. Standard tensile specimens (Figure 3.1) were punched out of these recrystallised strips. The final thickness of the strips was 0.5mm.

Table 3.1: Relevant properties of glasses and alloys

Composition	Thermal Expansion Coefficient $\times 10^{-6}, K^{-1}$	Softening point/ temperature for superplastic deformation $^{\circ}C$	ref.
<i>Glass</i>			
6.79 $Na_2O$ -29.93 $Al_2O_3$ -26.88 $B_2O_3$ -36.40 $SiO_2$ (wt% by analysis)	17.0	$\sim 520$	
<i>Metal</i>			
Zn - 16.22Al (wt% by analysis)	22.1	20 - 300	1, 2, 3

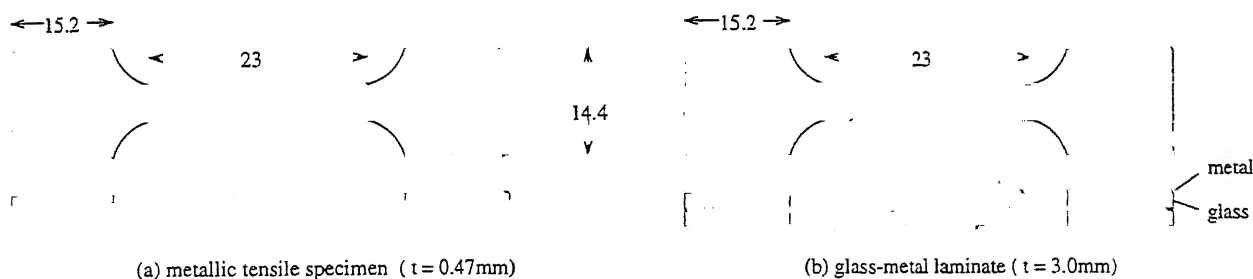


Figure 3.1: Plan and elevation of the tensile sample : (a) metallic; (b) glass-metal laminate.

### 3.3 Preparation of glass powder

A sodium alumino-boro-silicate glass having the % weight composition 6.79% $Na_2O$  29.93% $Al_2O_3$  26.88% $B_2O_3$  36.40% $SiO_2$  was taken for study. For melting the glass of above composition precisely weighed  $Na_2CO_3$ ,  $H_3BO_3$ ,  $Al_2O_3$  and  $SiO_2$  were taken. Sodium carbonate and boric acid give out  $Na_2O$  and  $B_2O_3$  respectively. These compounds were thoroughly mixed in ball-mill and then melted at  $\sim 1200^{\circ}C$  in a Pt-crucible. Molten glass was poured on a cooled copper plate (water was not used, since borate glass absorbs water

vapour and becomes opaque). The solid glass was crushed, milled and sieved through 53 $\mu$  mesh. The thoroughly dried glass powder was used as starting powder for the preparation of laminated composites. Since glass is extremely sensitive to rate of cooling, intricate dog-bone-shaped tensile sample can not be cast easily. So to study the deformation behaviour of glass cylindrical sample of glass was made. To cast cylindrical sample glass melted at 1250°C was poured in a heated graphite die with cylindrical cavity of diameter 9mm. These cylindrical sample was completely transparent and free from air bubbles.

### 3.4 Preparation of laminates

Laminated glass-metal composites were made by hot pressing in a 10T hot pressing unit (Electrofuel, Canada). A mild steel die with groove dimension matching with that of Zn-Al samples was taken. The die was properly cleaned and coated with BN suspension (BN acts as a lubricant). One Zn-Al sample was kept inside the die and then 1g of glass powder ( $Na_2O - Al_2O_3 - B_2O_3 - SiO_2$ ) was put over it. Then another Zn-Al strip and 1g of glass powder were put. Finally at the top a Zn-Al strip was kept. This combination of glass powder and metal was hot-pressed at 225°C for ~ 55min applying 1ton load. Thus we got glass-metal laminated composites.

### 3.5 Characterization of laminates

#### 3.5.1 Differential Thermal Analysis

Differential thermal analysis was done to find out the melting temperature and the temperature for the formation of crystalline phases using Shimadzu DTA-50. DTA was performed from the room temperature to 1000°C at the heating rate of 10°C/min.

#### 3.5.2 X-ray Diffraction

X-ray diffraction study (SIEFERT ISO DEBYEFLEX-1001) was done on glass powder obtained before and after hotpressing in the range 20° – 90° of 2 $\theta$  with a scanning speed of 3°/min using Cu target ( $\lambda = 1.54056, 20mA/30kV$ ). On the basis of DTA, the glass was heat-treated at three different temperatures and X-ray diffraction study was also

done on them. The glass powder obtained from the cylindrical glass sample tested at higher temperature was studied under X-ray diffraction.

### 3.5.3 Microstructural study

For optical microscopy, metal samples were fine polished and etched in fresh etchant(dilute HF for Zn-Al). Optical micrographs were taken at the magnification of 500X for Zn-Al and 100X using Lietz Metallovar optical microscope. Micrographs of Zn-Al and the laminates(especially their interface) were taken in backscattered mode using Jeol JSM-840A scanning electron microscope. Laminates were silver-coated before inserting into the microscope to prevent charging of the samples.

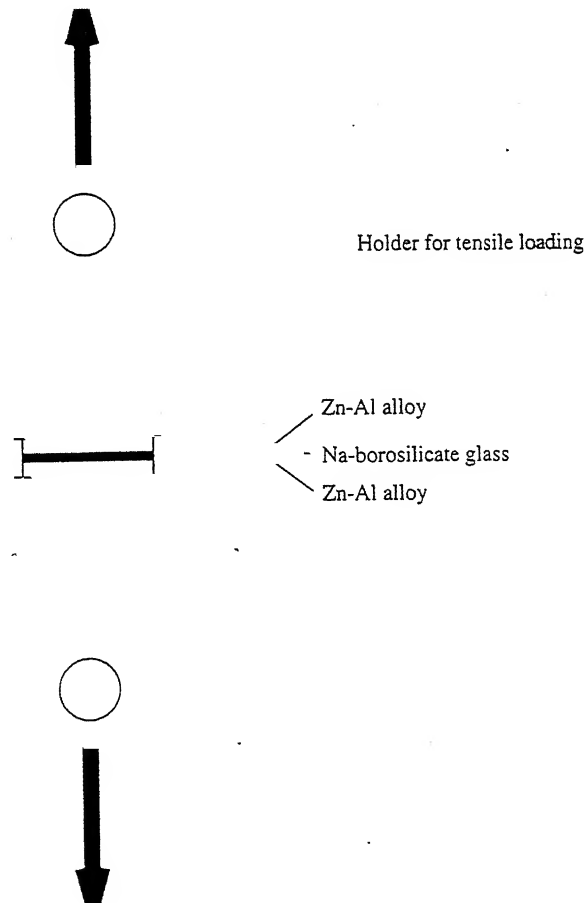


Figure 3.2: Interfacial bond strength measurement of Na-alumino-borosilicate glass-Zn-Al alloy laminate.

### 3.5.4 High temperature testing

High temperature tensile testing of alloy, glass and laminate was done using Instron 1195 and MTS (Material Testing System, model 810.12). For Zn-Al alloy and its laminates, Silicone oil bath was used at four different temperatures viz.  $160^{\circ}\text{C}$ ,  $180^{\circ}\text{C}$ ,  $200^{\circ}\text{C}$  and  $220^{\circ}\text{C}$ . Elongation-to-failure test, differential strain rate test and were carried out to characterise the materials. Interfacial bond strength of the laminate at room temperature was found out by loading the laminate interfacial plane perpendicular to the tensile loading axis as shown in the Figure 3.2. The cross-sectional area of the interface was  $12\text{mm}^2$ . The cross-head speed of loading was  $0.05\text{mm/min}$ .

## 3.6 Reference

1. G. Turner, J.Soc.Glass Tech., 18, 69, 1934. p32 - 66.
2. F. Porter, 'Zinc handbook', Mechanical Engineering Series, No. 73, 1991.
3. T.G. Langdon, Metall. TransA, Vol.13A, No.5, p.689-701.
4. K.A. Padmanabhaan and G.J. Davis, 'Superplasticity', Springer-Verlag, 1980.

# Chapter 4

## Results and discussion

### 4.1 Introduction

Glass is extremely brittle material with low fracture resistance. Since glass is isotropic in nature crack generally nucleates from surface or interface between glass and metal or crystalline inclusions in glass[1]. Once a crack is initiated it propagates very fast. In glass-metal laminates, stresses responsible for nucleation of cracks are dictated by many factors. In such laminates, the coefficient of thermal expansion (CTE) of metal is high, CTE mismatch stresses can easily nucleate crack in glass. In some extreme cases, fracture can readily occur in the glass matrix. Hence to control the stresses built up in glasses the thermal expansion properties of both have to be chosen carefully. Thermal expansion coefficient match between glass and metal ensures stress-free glass when the joint is cooled. In reality a perfect match between the thermal expansion properties of glass and metal is not possible. One has always to contend with some residual stresses in the glass-metal bond. Although it is possible to choose combinations of glass and metal in which the expansion curves of the two materials are close over the entire temperature range (i.e. from room temperature up to the annealing temperature of the glass), batch to batch variations in the compositions of the materials occur and consistency would be difficult. When the glass-metal bond is cooled, initially the glass viscosity is too low for any permanent stress to arise. But when the glass viscosity reaches a value of approximately  $10^{12}$  Pa·s, the rate of stress release in the glass by viscous flow is such that some stress begins to develop. As the temperature falls further, glass behaves as an elastic solid and, further stress release is not possible. This temperature is known as set point and designated as  $T_s$ . If the differential free contraction ( $\delta$ ), it is defined as the difference between the free contraction of glass and metal per unit length in the direction parallel to

the interface when they had not been bonded together;  $\delta = (\alpha_{metal} - \alpha_{glass}) \cdot (T_s - T)$ ,  $T$  is any temperature,  $T < T_s$ ) is positive i.e.  $\alpha_{metal}$  is greater than  $\alpha_{glass}$ ; then in a metal-glass-metal sandwich bond contracting together, a tensile stress will set up in metal and a compressive stress in glass. Glass can withstand very high compressive stress but fails easily in tension. But according to a thumb rule, any stress developed in the glass should be less than 10MPa[2]. Thus in the present study, a glass is chosen which is having thermal expansion coefficient less than that of the metal. The glass softening point was another criterion for glass selection because the viscosity of glass has to be sufficiently low in the temperature range where the metal can flow easily. Any crystallisation hinders the flow behaviour of glass. Initially, extensive search was done to select suitable glass system with appropriate thermal expansion coefficient and  $T_g$  such that glass and metal deform co-operatively. Regarding simultaneous deformation of glass/metal, in addition to  $\alpha$  and softening point, various other factors are important : (a) Elastic moduli of glass and metal; (b) Microstructure of metal; very fine grain structure is recommended for superplasticity; (c) Presence of crystallites in glass; these suspensions hinder the flow of glass at higher temperature; (d) Interfacial strength; good interfacial bonding is required to prevent delamination; (e) Nature of loading; it determines whether the component is experiencing tensile/compressive stress. Compressive strength of glass is higher than its tensile strength; (f) Internal flaws; the glass has to be free from inclusions, porosity etc. otherwise crack generates from them; (g) Abrasion and friction; metal sheets should cover the glass in a sandwich bond otherwise frictional forces of grip for testing destroy the glass.

## 4.2 Characterisation of laminate

The glass-metal laminate was prepared by hot-pressing (described in chapter 3). The characterisation of laminate is required as this enables us to make remarks on its composite nature. Its interface and the flow behaviour at higher temperature were characterised as below.

### 4.2.1 Interface of laminate

In a composite material, interface between its components is the most important part of it and needs excessive care. The interface plays an important role in the mechanical performance of the composite. In glass-metal laminate, brittle glass is reinforced with



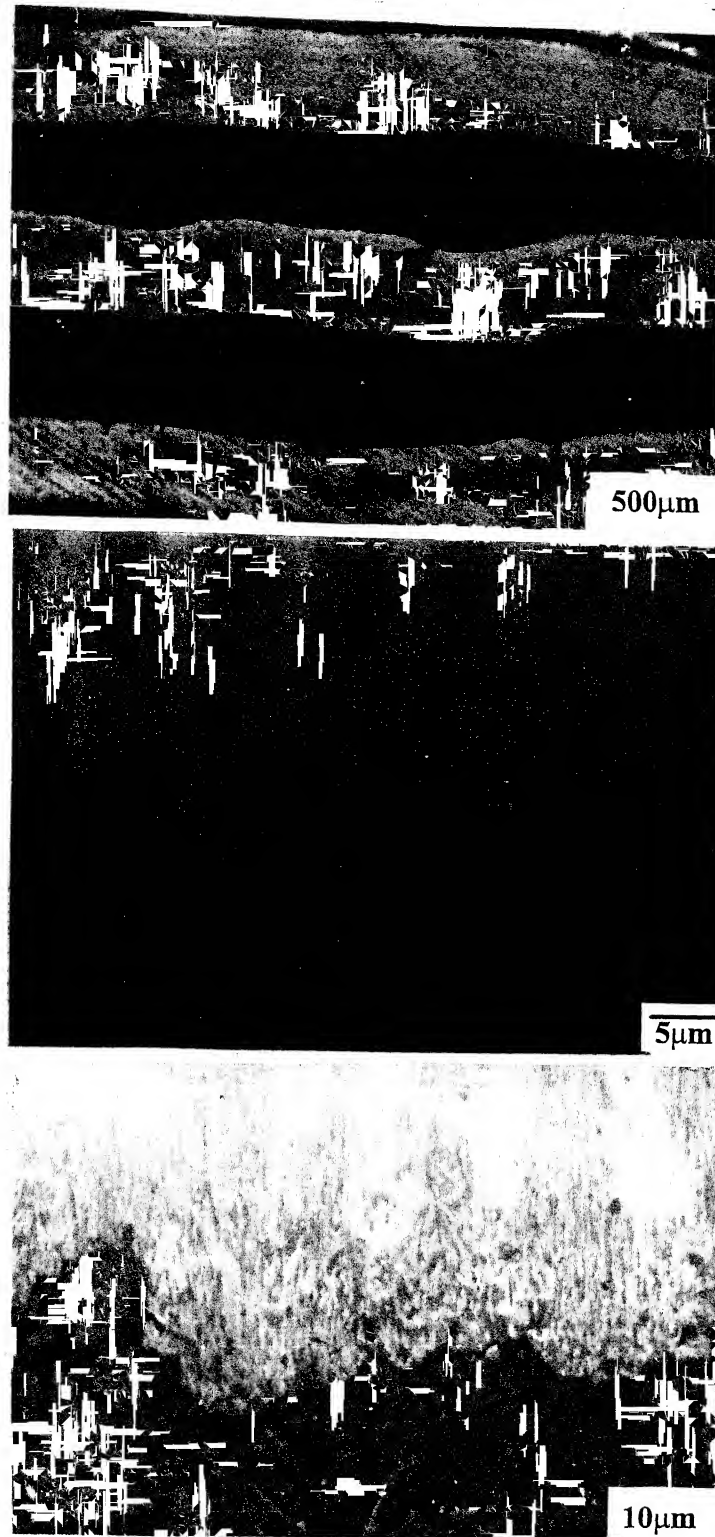


Figure 4.1: Micrographs of laminate showing different layers of components and their interface.

ductile metal. So unlike ceramic fibre reinforced ceramic composite, ductile layer reinforced ceramic composite should have strong interface between its components. Strong interface can arrest a crack while a weak interface is very much prone to delamination failure. The interface can be characterised qualitatively by microstructural study and it (Figure 4.1) shows layers of glass sandwiched within the layers of metal without any presence of intermediate phase at the interface. The interface is a mechanical interlocking of the asperities of both glass and metal. The interfacial bond strength was determined by a simple method (Figure 3.2). The sandwich laminate of glass and metal is bonded to the holder by adhesive and it is loaded in uniaxial tensile mode at the lowest possible cross-head velocity, provided the adhesive bond strength is higher than the laminate bond strength. At room temperature the bond strength is 0.97 MPa. Such a low value confirms again the mechanical interlocking at the interface. However, the interfacial bond strength can be increased by using interlayers, pre-oxidising the metal layers, deposition of a compound or element on the glass before hot-pressing[3], hot-pressing at higher temperature to ensure higher rate of diffusion in either layers.

#### 4.2.2 Flow behaviour of laminate

The laminate was tested at four different temperatures (160°C, 180°C, 200°C, 220°C) in tensile mode. Firstly, strain rate change tests were carried out at each temperature to find out the strain rate sensitivity indices ( $m$ ) at various temperatures. Strain rate ( $\dot{\epsilon}$ ) and flow stress ( $\sigma$ ) were calculated using a standard method[4]. Double logarithmic plot of flow stress vs. strain rate (i.e.  $\log \sigma - \log \dot{\epsilon}$ ) are shown in Figure 4.2. The flow stress decreases with the increase in temperature - a common feature of superplastic flow which shows that the change from normal to superplastic flow of deformation is gradual and there is no sudden onset of temperature for superplasticity[5]. It is observed that the stress required for straining in case of laminate is very low as compared to Zn-Al alloy (for Zn-Al alloy, discussed in section 4.4.2); for example, at 220°C and  $\dot{\epsilon} = 10^{-2}$ ,  $\sigma = 4\text{MPa}$  for laminate while  $\sigma = 20\text{MPa}$  for the alloy. This can be explained using rule-of-mixtures assuming iso-strain behaviour. The glass behaves like an elastic solid at 220°C and its strength at this temperature is very low (its room temperature tensile strength is  $\sim 50\text{MPa}$ ). Its volume fraction is 0.53. On the other hand, the metal has much higher stress value at that temperature as compared to glass (its room temperature tensile strength is measured as 190MPa), but its volume fraction is 0.47. At same strain, rule-of-mixtures gives a stress value for laminate which is much lower than that of Zn-Al alloy. The slope of this  $\log \sigma - \log \dot{\epsilon}$  curves is the strain rate sensitivity ( $m$ ) at

that temperature. Strain rate sensitivity varies with strain rate. So, a non-linear function

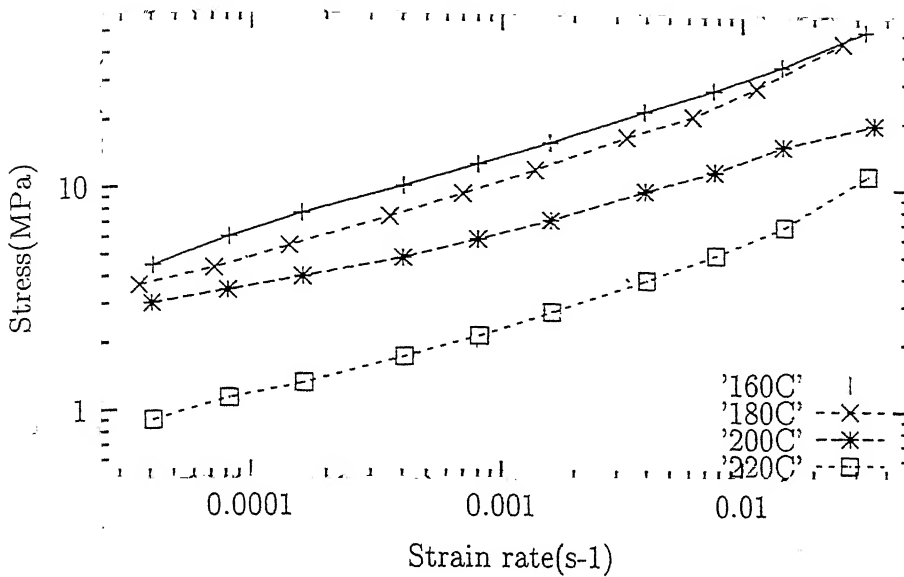


Figure 4.2: True stress-true strain rate plot for laminate at 160°C, 180°C, 200°C and 220°C

(evaluated by least-square method) is fitted to each curve and the variation of  $m$  is plotted against strain rate (Figure 4.3). The variation of  $m$  value at 160°C is very less; therefore corresponding curve in Figure 4.2 is a straightline with average slope i.e.  $m = 0.353$ . But at 220°C,  $m$  sharply increases from low strain rate to high strain rate and a maximum value of 0.55 at  $\dot{\epsilon} = 2 \times 10^{-2}$  was achieved i.e. high strain rate is favourable for deformation of laminate. Because, high temperature (i.e. 220°C) facilitates the diffusion process within the alloy (grain boundary diffusion and bulk diffusion) as well as in the glass (atomistic diffusion). Since lower stress is required for laminate deformation, the constitutive equation for superplasticity ( $\sigma = K\dot{\epsilon}^m$ ) gives out that the strain rate should decrease or shift to lower value, provided  $m$ ,  $\epsilon$ ,  $T$ ,  $d$  remain constant. This theoretical inference is proved by experimental data shown in Figure 4.2. Secondly, elongation-to-failure tests were carried out at various temperatures (160°C, 180°C, 200°C, 220°C) and at different initial strain rate. A comparison of elongation values at those temperatures and at same initial strain rate is shown in Figure 4.4. There is a trend of increasing elongation values with temperatures. At 220°C, maximum % elongation was obtained at that strain rate. This confirms the inference from Figure 4.2 that superplastic deformation is favourable at that temperature. The % elongations at various temperatures and initial strain rates are tabulated in Table 4.1.

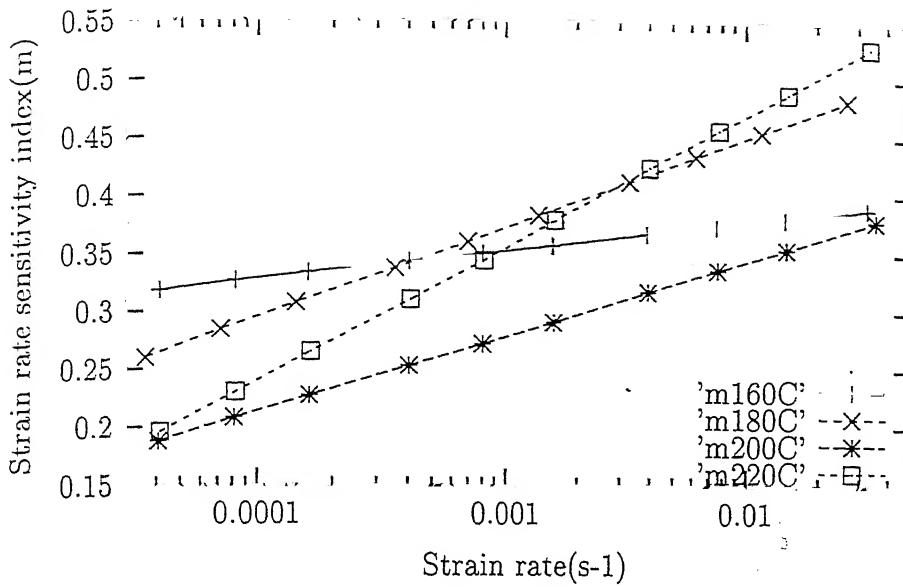


Figure 4.3:  $m - \log \epsilon$  plot for laminate at 160°C, 180°C, 200°C and 220°C

At a particular temperature, % elongation value changes with strain rate and the form of curve is similar to Figure 2.13.

Table 4.1: % elongation of laminate at various temperature and initial strain rate

Temperature(°C)	Initial strain rate( $s^{-1}$ )	% elongation
160	$4.14 \times 10^{-4}$	90
180	$4.63 \times 10^{-4}$	190
	$2.61 \times 10^{-3}$	130
200	$1.57 \times 10^{-4}$	90
	$3.65 \times 10^{-4}$	215
	$3.62 \times 10^{-3}$	155
220	$3.50 \times 10^{-4}$	165
	$4.38 \times 10^{-4}$	335
	$3.33 \times 10^{-3}$	160
	$3.47 \times 10^{-3}$	290

## Zn-Al/Glass Laminated composite

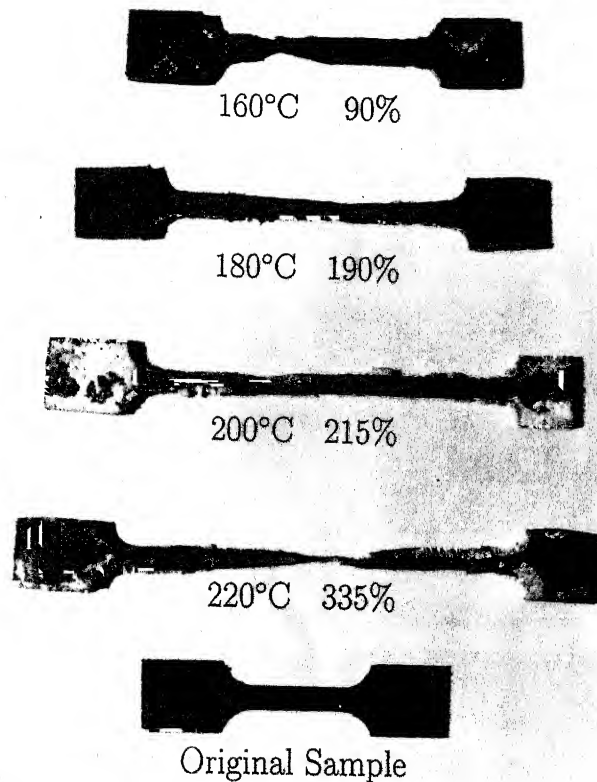


Figure 4.4: Comparison of % elongation values of laminate.

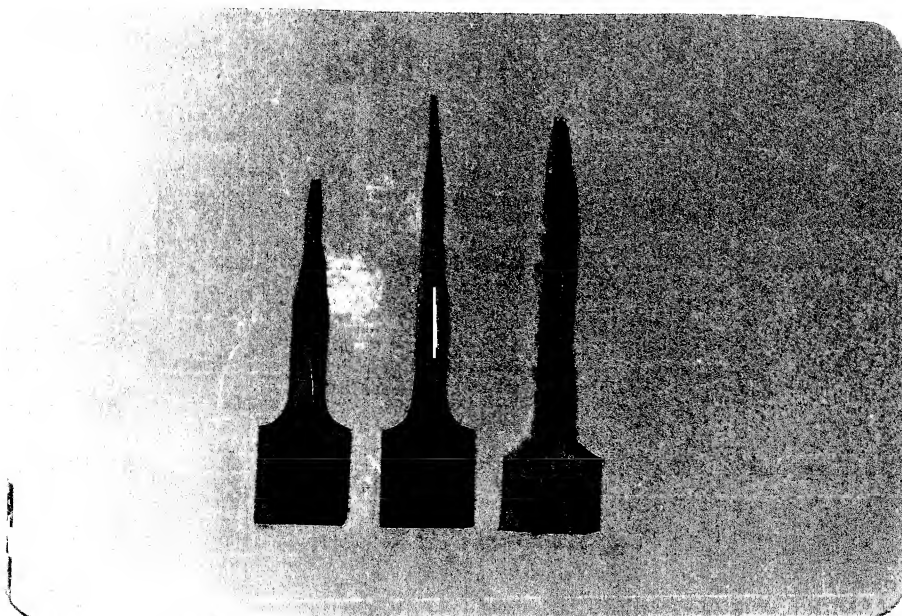


Figure 4.5: Gradual failure of metal layers in laminate.

The laminate shows no visible interlaminar failure when small amount of strain was given to it. When it was unloaded after a small straining, no delamination was observed. But after appreciable amount of straining, the microcracks, previously nucleated in glass due to thermal expansion coefficient mismatch between crystalline phase in glass and residual glass and thereby stress-concentration at those points, propagated across the glass layer. So, the glass layers are cracked in a plane perpendicular to tensile axis of loading. Delamination occurred at higher strains and the metal layers dictated the overall deformation till they failed. The metal layers did not fail simultaneously, but one after another (Figure 4.5). This may be due to interlaminar frictional force offered by brittle glass to metal layers or some intrinsic defect within the metal layer itself, which changes its position and offers stress-concentration at a point or the cavitation accommodation process was hindered by some internal defects. Activation energy for laminate deformation is calculated from the plot  $\ln \sigma$  vs.  $1/T$  using

$$\dot{\epsilon} = A d^{-p} \sigma^n \exp\left(\frac{-Q}{RT}\right)$$

to verify the predominant physical process. The average activation energy is 161 KJ/mol which is very much higher than that of superplastic deformation of metal (see section 4.4.3). The metal seemed to dictate the deformation, but discrepancy comes since, (a) the activation energy equation can be applicable only when temperature interval is small; (b)  $n$  varies with temperature; (c) constant  $A$  contains a number of temperature dependent terms; (d) grain size is a function of temperature; (e) measurement should be made from modulus compensated stress; (f) the exact form of this equation is not known; (g) above all, interfacial energy contribution is not known. To have better understanding of laminate deformation, the individual components namely glass and Zn-Al alloy were also characterised.

### 4.3 Characterisation of glass

A borate glass of composition (6.79%  $Na_2O$ -29.93%  $Al_2O_3$ -26.88%  $B_2O_3$ -36.40%  $SiO_2$ ) was chosen for this study. Borate glass is low-melting glass.  $B_2O_3$  is a network forming oxide; it forms strong glasses. It is reported that Zn-Al alloy shows superplasticity in the temperature range 20 – 300°C. So the glass should soften in that temperature range. Generally the softening point of borate glass is very low compared to silicate glasses. So it is presumed that the glass and metal will deform simultaneously without fracture. Secondly, the thermal expansion coefficient of glass is less than that of metal ( $22.1 \times 10^{-6}/C$ ). So during cooling of the glass/metal bond, a compressive stress is set up in glass which may be tolerable to glass. Before evaluating the response of glass in the glass/metal laminate at higher temperature,

the individual deformation behaviour of glass is required to be known. Mechanical tests of glass at higher temperature were done to evaluate the flow behaviour of glass. DTA and X-ray diffraction studies were taken up to find out the presence of crystals, if any, in the glass.

### 4.3.1 DTA and X-ray diffraction

Chemical reaction or structural changes within a glass are accompanied by the evolution or absorption of energy in the form of heat. When a glass crystallises, an exothermic effect occurs since the free energy of the regular crystal lattice is less than that of the disordered glassy state. Conversely, the melting of a glass or a crystal gives rise to an endothermic effect. Differential thermal analysis (DTA) is a technique which enables reactions or phase transformations to be studied for substances at high temperature. DTA of glass was done to study its crystallisation using a reference neutral body ( $Al_2O_3$ , which does not exhibit endothermic or exothermic effect) when temperature of the both was increased at the rate of  $10^\circ C/min$  from room temperature to  $1000^\circ C$ . As the temperature was increased dips were observed at  $249.33^\circ C$  and  $520.87^\circ C$ , while a peak was seen at  $929.39^\circ C$  (Figure 4.6(a)). The first dip (corresponding to  $249.33^\circ C$ ) may be due to slight absorption of heat when annealing point (i.e. stress-relieving point) of the glass is reached. It implies that there should not be any chance of crystallisation of the glass. To verify this fact, the glass was heat-treated at  $280^\circ C$  for 1 hour and DTA (Figure 4.6(b)) was carried out of the glass. It shows a steady peak i.e. crystallisation of glass has occurred and this was supported by the X-ray diffraction (Figure 4.7(b)) study performed on the same glass sample. But a larger dip was seen at  $520.87^\circ C$ . Similarly, in this case, the glass was heat-treated at  $550^\circ C$  and DTA was done and X-ray diffraction study was carried out. DTA (Figure 4.6(c)) and X-ray diffraction plot (Figure 4.7(c)) shows presence of crystalline phase in the glass. X-ray plots show presence of same crystal as before. But in this case, we can conclude from greater extent of dip in DTA plot (Figure 4.6(a)) that the residual glass might have been melted absorbing some amount of heat. Sharp hump at  $929.39^\circ C$  (Figure 4.6(a)) proves the complete crystallisation of the glass. And this is supported by a DTA (Figure 4.6(d)) of the glass heat-treated at  $1000^\circ C$  for 1 hour. X-ray diffraction plots (Figure 4.7(d)) also shows presence of crystalline phase of same nature as before. The crystalline phase melts completely at around  $1200^\circ C$ . The glass was melted at  $1200^\circ C$  and then cooled and X-ray diffraction study was done for it. The X-ray plot (Figure 4.7(a)) shows diffuse X-ray diffraction patterns with complete absence of sharp lines. This implies that the whole system of crystalline phase and glass was melted at around  $1200^\circ C$ .

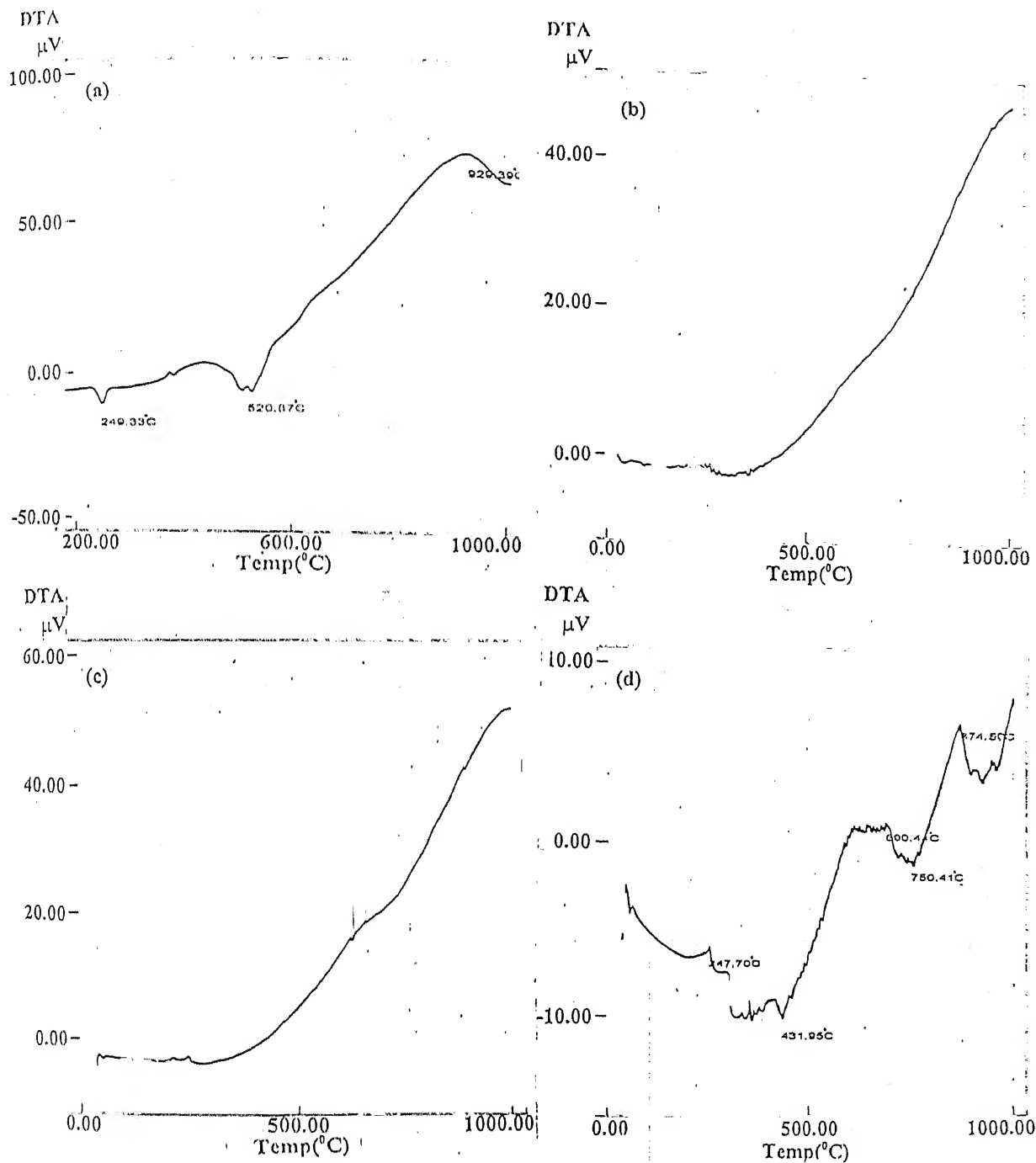


Figure 4.6: DTA result of (a) original glass powder, and glass heat-treated for 1 hour at (b) 280 $^{\circ}\text{C}$ , (c) 550 $^{\circ}\text{C}$  and (d) 1000 $^{\circ}\text{C}$ .



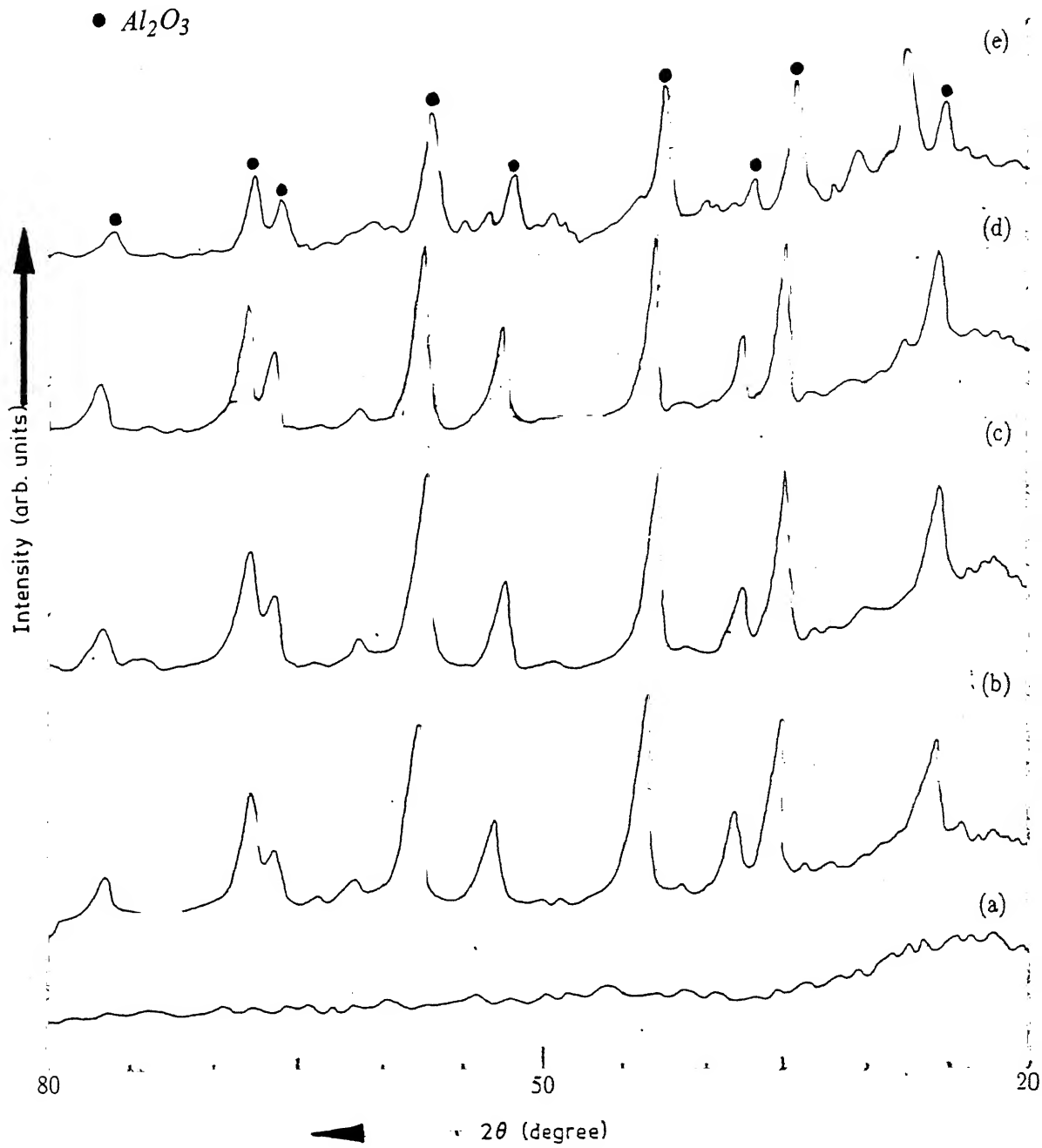


Figure 4.7: X-ray diffraction plots of the glass powder : (a) tested in compression, (b) heat-treated at 280°C, (c) heat-treated at 550°C and (d) heat-treated at 1000°C, (e) taken from laminate.

### 4.3.2 Flow behaviour of glass

Since glass is extremely brittle, handling, preparation and testing of tensile sample of glass is very difficult. However, carefully controlling the cooling rate of the glass casting of glass in a definite shape is possible. So, simple cylindrical sample of glass was made and used for high temperature mechanical testing. To investigate the flow behaviour of the glass, cylindrical sample (height/diameter = 2) of glass was tested in compressive mode.

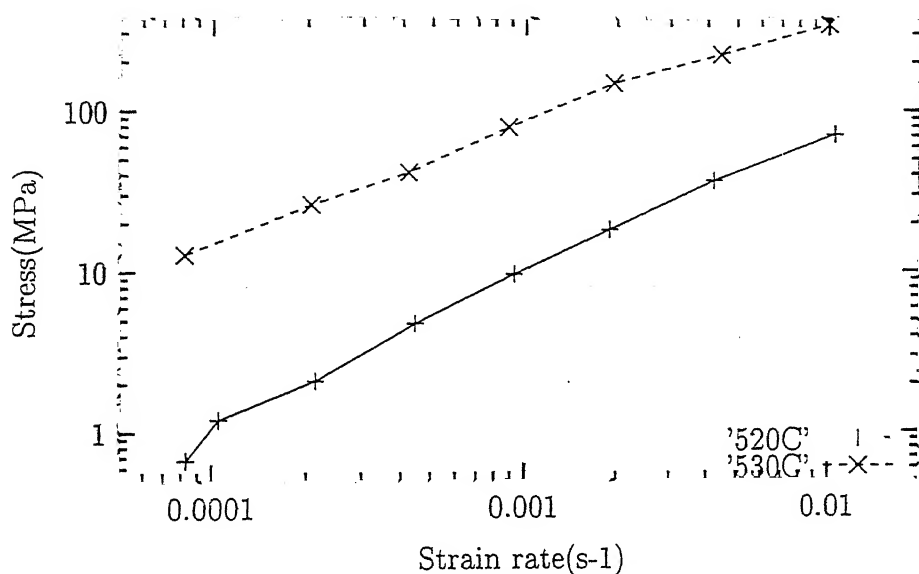


Figure 4.8: True stress-true strain rate plot for Sodium aluminoborosilicate glass at 520°C and 530°C

Though it is assumed that the glass softens at very low temperature, it is found out that the glass behaves like perfect elastic solid in the temperature range of 20 – 300°C. That is, it does not show any flow behaviour in the aforesaid range of temperature. But at 520°C and above, it behaves like plastic material and shows appreciable Newtonian flow characteristics. Assuming that the glass obeys  $\sigma = K\dot{\epsilon}^m$ , the strain rate sensitivity index of flow stress is found from the slope of the  $\log\sigma$ - $\log\dot{\epsilon}$  plot (Figure 4.8). The values of strain rate sensitivity index are close to unity and it implies high ability of glass to resist necking and flow like a perfect Newtonian fluid. A non-linear function is fitted to  $\log\sigma$  -  $\log\dot{\epsilon}$  curves and subsequently the change of  $m$  with strain rate is plotted (Figure 4.9).

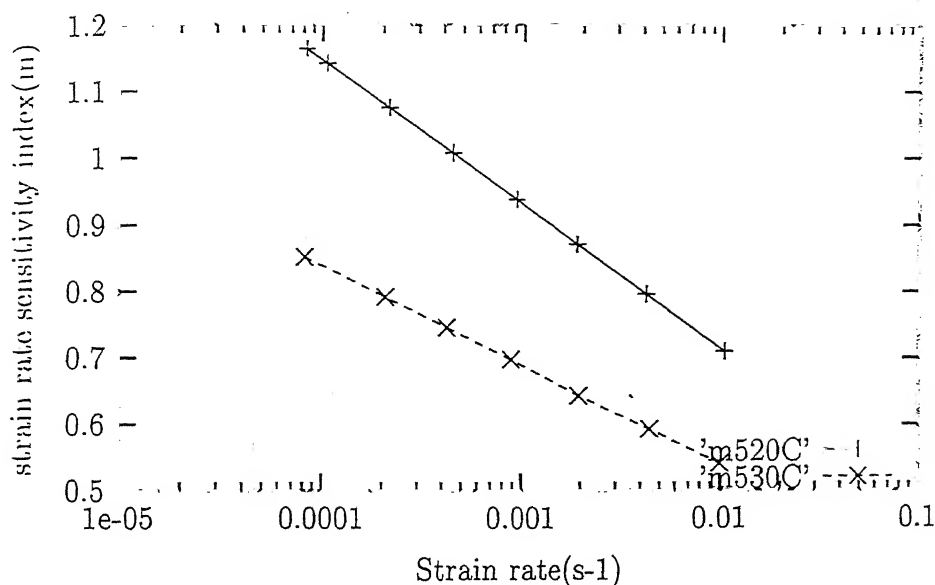


Figure 4.9:  $m - \log \dot{\epsilon}$  plot for Sodium aluminoborosilicate glass at 520°C and 530°C

## 4.4 Characterisation of Zn-Al alloy

### 4.4.1 Microstructural Study

Since grain size and the stability of grain size are important criteria for superplasticity in a metallic material, microstructural study is needed for Zn-Al alloy. Sample taken from rolled and subsequently recrystallised Zn-Al sheet was metallographically prepared for microstructural study. Polished sample was etched using dilute HF. Since the average grain size of this alloy is very less ( $< 5\mu\text{m}$ ) optical microscope can not be used for grain size measurement. Micrographs were taken by Scanning electron microscope in back-scattered mode and line-intercept method was applied for measuring the grain size. The grain size is  $2\mu\text{m}$  in the rolling plane Figure 4.10(a). The micrographs taken in the rolling plane and other two perpendicular transverse planes are shown in Figure 4.10.

### 4.4.2 Flow behaviour of Zn-Al alloy

The superplastic Zn-Al alloy was tested at four different temperature e.g. 160°C, 180°C, 180°C, 200°C, 220°C in tensile mode. Firstly, strain rate change tests were carried out at each temperature to find out the strain rate sensitivity index of flow stress at

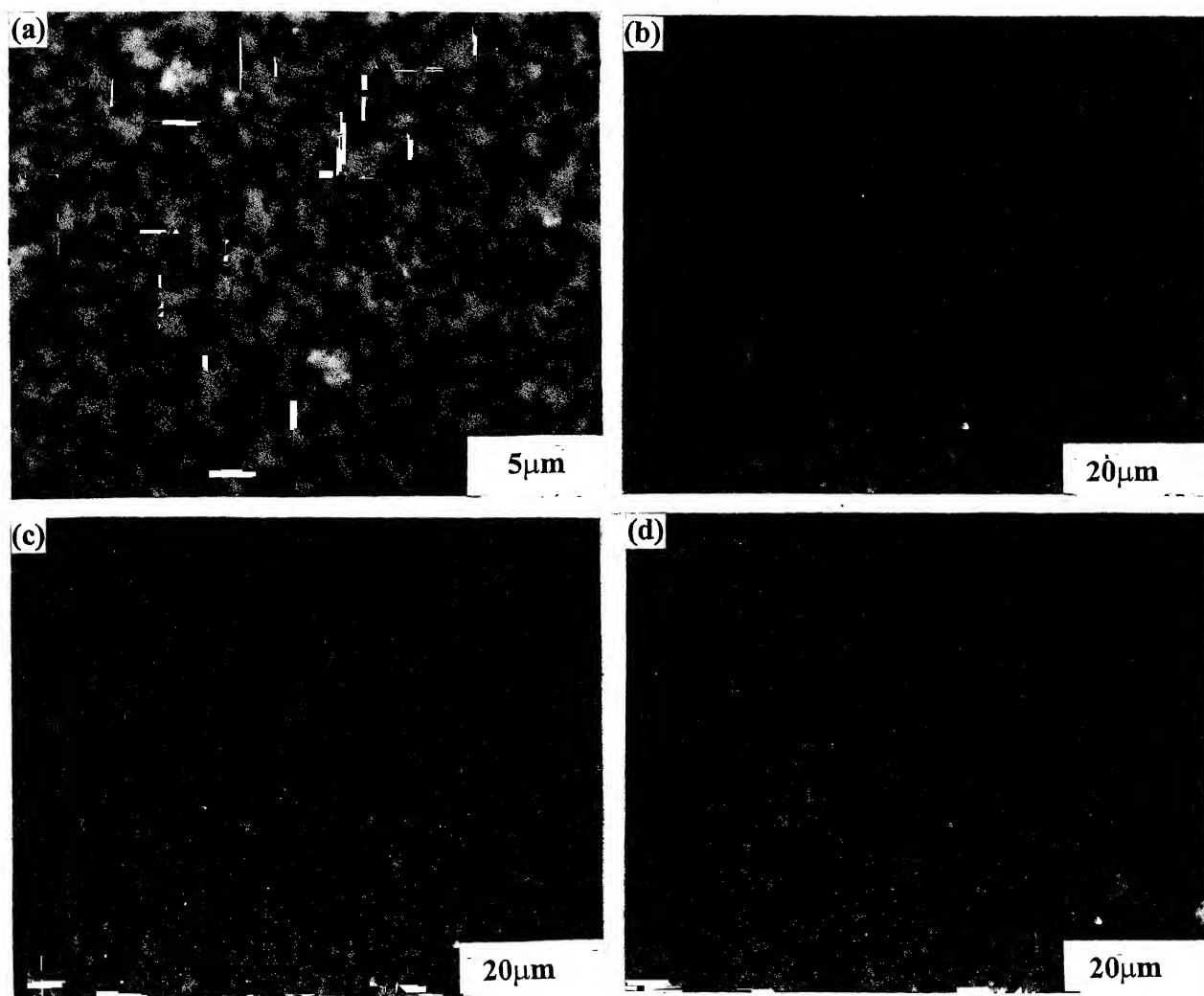


Figure 4.10: Microstructure of Zn-Al alloy (a) recrystallised; (b) rolling plane; (c) & (d) other two transverse plane.

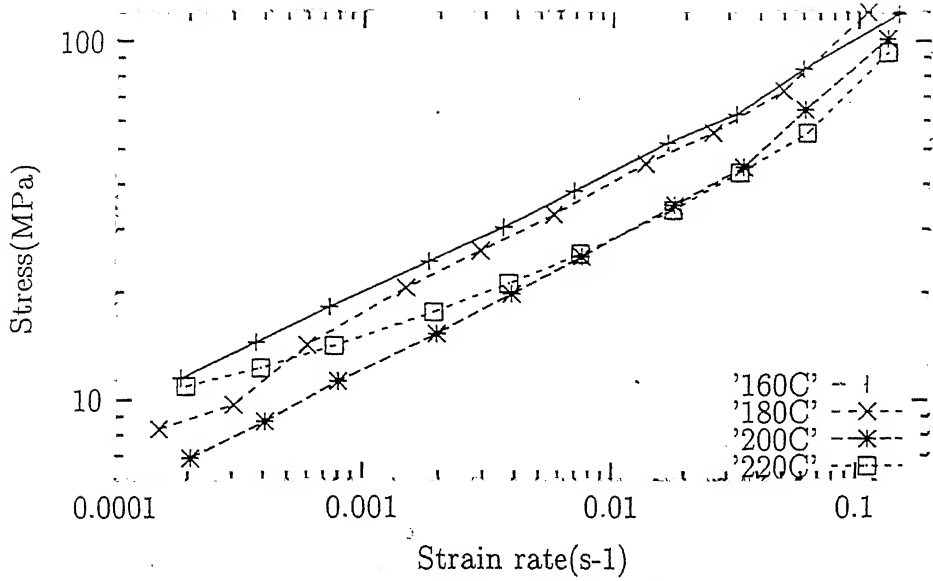


Figure 4.11: True stress-true strain rate plot for Zn-Al at 160°C, 180°C, 200°C and 220°C

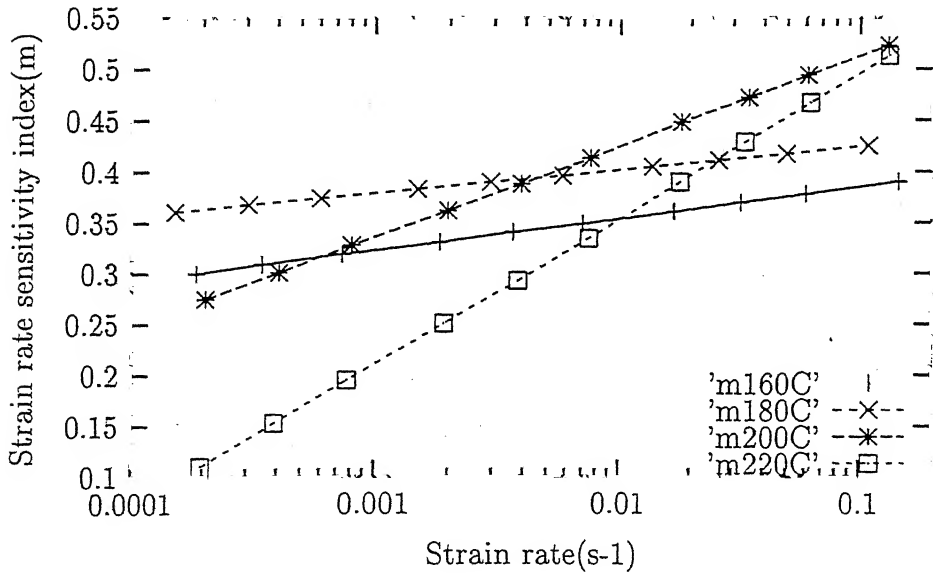


Figure 4.12:  $m - \log \dot{\epsilon}$  plot for Zn-Al at 160°C, 180°C, 200°C and 220°C

various temperature. Cross-head velocity was increased gradually to increase strain rate and corresponding flow stress at a particular temperature. Strain rate( $\dot{\epsilon}$ ) and flow stress( $\sigma$ ) were calculated from standard method[3]. Double logarithmic plot of Flow stress and strain rate are shown in Figure 4.11. The slopes of theses curves do not change much except in the case of 220°C. A non-linear function is fitted in each curve and the change of slope of  $\log \sigma - \log \dot{\epsilon}$  i.e.  $m$  is plotted against strain rate shown in Figure 4.12 which shows the change of  $m$  values

over the

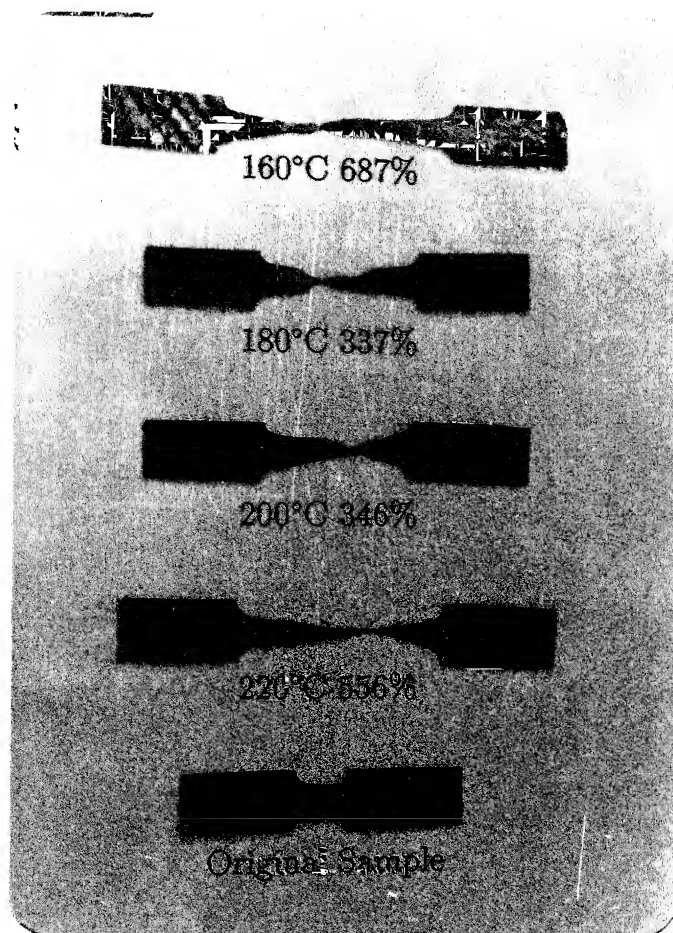


Figure 4.13: Comparison of % elongation values of alloy.

given strain rate range. Change in strain rate sensitivity index at  $160^{\circ}\text{C}$  and  $180^{\circ}\text{C}$  is not much and remain within 0.3 to 0.35 and 0.35 to 0.4 respectively. But at  $220^{\circ}\text{C}$  the  $m$ -value changes severely from 0.1 at  $\dot{\epsilon} = 2 \times 10^{-4}$  to 0.5 at  $\dot{\epsilon} = 10^{-1}$ . This implies that the superplastic deformation in Zn-Al is very much favourable at  $220^{\circ}\text{C}$  as neck resistance is very high. High value of strain rate sensitivity index of flow stress implies high ductility at that temperature or high resistance to plastic instability. That is, the metal can be deformed at ease applying a nominal stress at a suitable temperature. Secondly, elongation-to-failure tests were carried out at various temperature ( $160^{\circ}\text{C}$ ,  $180^{\circ}\text{C}$ ,  $200^{\circ}\text{C}$ ,  $220^{\circ}\text{C}$ ) and the strain rate. A comparison of elongation at various temperature and at almost same strain rate is shown in Figure 4.13. % elongation at a temperature increases gradually to a maximum and

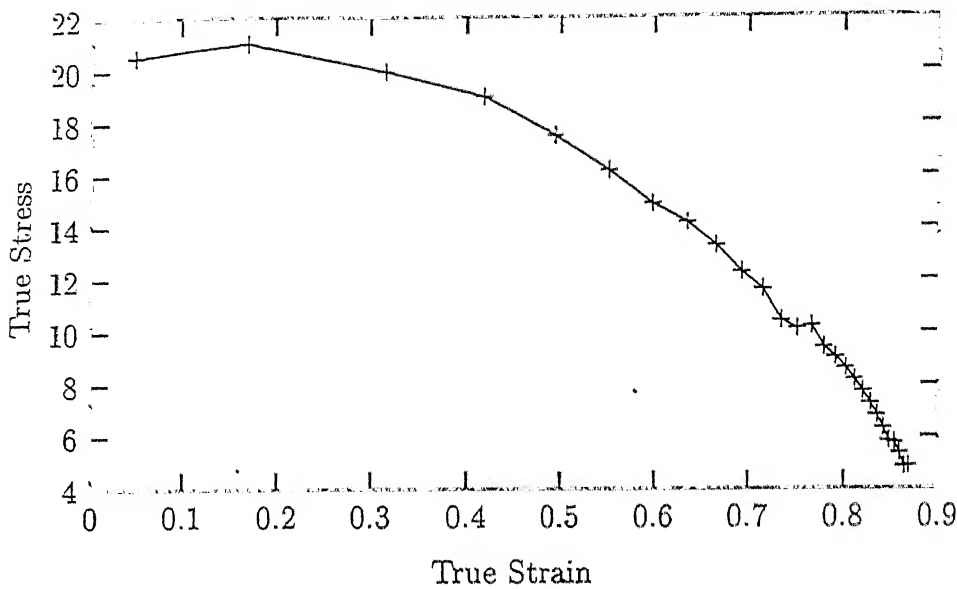


Figure 4.14: True stress-true strain plot for Zn-Al at 160°C with cross-head velocity 0.5mm/min, gauge length 3.9mm

then decreases with increasing strain rate. An empirical idea can be drawn from true stress-true strain plot at a particular temperature and cross-head velocity. Maintaining constant strain rate during elongation-to-failure test is not easy because the actual cross-sectional area decreases gradually. For superplastic material true stress-true strain plot should be a horizontal straight line. Any increase in stress implies grain growth but decrease shows initiation of cavitation[3]. Figure 4.14 shows gradual decrease in the stress value indicating onset of cavitation. Therefore, the metal remains stable during test, but ultimately fails by cavitation. Activation energy for superplastic deformation is calculated using same expression used for activation energy calculation for deformation of laminate.  $n \log \sigma$  is plotted against  $\frac{1}{T}$  and  $Q$  is calculated out from the slope of the curves. The activation energy was found out to be 120 KJ/mol.

## 4.5 References

1. E.R. Lawn and T.R. Wilshaw, 'Fracture of brittle solids', Cambridge University Press, Cambridge, 1975.
2. H. Rawson, 'Properties and application of glass', Glass Science and Technology, 3, Elsevier, 1980.

3. T.S. Oh, R.M. Cannon and R.O. Ritchi, J.Am.Ceram.Soc., Vol.70, 1987, p.c352.
4. J.Pilling and N.Ridley, 'Superplasticity in Crystalline Solids', The Institute of Metals, 1989.
5. A.Ball and M.M.Hutchison, J.Met.Sci., Vol.3, 1969, p.691.



# Chapter 5

## Summary

From the present study on the high temperature deformation of sodium aluminoboro-silicate glass, eutectoid zinc-aluminium alloy, and their laminate, following conclusions can be drawn :

1. Very small stress is required for laminate deformation. High values of strain rate sensitivity index( $m$ ) and % elongation are obtained at 220°C. Activation energy is higher than that of metal. Delamination occurs at higher strain. The interface bond strength is poor and the bonding is mechanical interlocking. The glass within the laminate crystallises.
2. The glass is elastic at the testing temperatures used for laminate. Above 520°C it shows inelastic deformation with strain sensitivity index as high as unity.
3. The alloy is very fine-grained and showed pronounced superplasticity at various temperatures used for laminate testing. There are no strain induced grain growth in the alloy. It fails when cavitation accommodation is no more possible.
4. Above all, a good glass-metal laminate with simultaneous deformation characteristics can be made by strongly bonding a glass with low-softening point and high glass transition temperature and a superplastic metal with higher thermal expansion coefficient.

## Chapter 6

### Suggestion for future work

So far, glass-metal bonding has been used in lamp manufacturing, enamelling of metallic objects, metallizing of ceramic substrate and as substrate in electronic packaging. Mainly refractory metals are used in glass-metal seals. But if a superplastic metal is incorporated in glass-metal laminate, a highly deformable composite can be made. Intimately bonded glass-metal laminate can be deformed to a large extent and complicated shapes can be made. So following suggestions are made from the above work :

1. Choosing suitable components of laminate, high temperature tensile testing can be done in the superplastic deformation temperature range of metal provided softening point of the glass is in the same range. Mathematical modelling is required to find out a deformation mechanism for laminate which matches with experimental study.
2. Using different interlayers suitable for the components of the laminate the interfacial bond strength can be determined and compared with each other. Design of test to determine interfacial bond strength in glass-metal laminate is required.
3. Using finite element method the stress concentration point can be found out and this give probable location of crack nucleation.